CZECH TECHNICAL UNIVERSITY

Faculty of electrical engineering

Department of electrotechnology

Diploma thesis

FIBER-REINFORCED CONCRETE BEHAVIOR IN MAGNETIC FIELD

Veranika Karpuk

Supervisor: Ing. Karel Künzel, CSc.

Study program: Electrical Engineering, Power Engineering and Management

Specialization: Electric drives

21.05.2021

ZADÁNÍ DIPLOMOVÉ PRÁCE

I. OSOBNÍ A STUDIJNÍ ÚDAJE

Příjmení: **Karpuk** Jméno: **Veranika** Osobní číslo: **457247**

Fakulta/ústav: **Fakulta elektrotechnická**

Zadávající katedra/ústav: **Katedra elektrických pohonů a trakce**

Studijní program: **Elektrotechnika, energetika a management**

Specializace: **Elektrické pohony**

II. ÚDAJE K DIPLOMOVÉ PRÁCI

Název diplomové práce:

Chování drátkobetonu v magnetickém poli

Název diplomové práce anglicky:

Fiebre reinforced concrete behaviour in magnetic field

Pokyny pro vypracování:

1. Seznamte se s problematikou vláknové výztuže betonových směsí a možnostmi orientace drátků v drátkobetonu
2. Seznamte se s experimentálním pracovištěm pro orientaci drátkové výztuže v magnetickém poli
3. Sestavte model experimentálního pracoviště metodou konečných prvků.
4. Ověřte funkčnost modelu a porovnejte s experimentálním pracovištěm.
5. Vyšetřete závislost momentu působícímu na feromagnetické vlákno v závislosti na rozměrech a dalších parametrech drátku.
6. Vyšetřete vliv dalších parametrů měřicí sestavy.
7. Upravte a ověřte model pro další experimentální sestavy.

Seznam doporučené literatury:

1. Takáčová Kristýna. Studie orientace vláken v cementovém kompozitu pomocí magnetického pole [Bakalářská práce]. [Praha]: ČVUT v Praze, fakulta stavební; 2017.
2. Takáčová Kristýna. Vývoj a testování přístroje pro cílenou orientaci vláken v cementových kompozitech pomocí elektromagnetického pole [Diplomová práce]. [Praha]: ČVUT v Praze, fakulta stavební; 2020.
3. Wijffels MJH, Wolfs RJM, Suiker ASJ, Salet TAM. Magnetic orientation of steel fibres in self-compacting concrete beams: Effect on failure behaviour. Cem Concr Compos. 2017 Jul 1;80:342–55.

Jméno a pracoviště vedoucí(ho) diplomové práce:

Ing. Karel Künzel, CSc., katedra elektrotechnologie FEL

Jméno a pracoviště druhé(ho) vedoucí(ho) nebo konzultanta(ky) diplomové práce:

Datum zadání diplomové práce: **19.09.2019** Termín odevzdání diplomové práce: **21.05.2021**

Platnost zadání diplomové práce: **30.09.2021**

Ing. Karel Künzel, CSc. podpis vedoucí(ho) práce	podpis vedoucí(ho) ústavu/katedry	prof. Mgr. Petr Páta, Ph.D. podpis děkana(ky)

III. PŘEVZETÍ ZADÁNÍ

Diplomantka bere na vědomí, že je povinna vypracovat diplomovou práci samostatně, bez cizí pomoci, s výjimkou poskytnutých konzultací. Seznam použité literatury, jiných pramenů a jmen konzultantů je třeba uvést v diplomové práci.

. Datum převzetí zadání

Podpis studentky

ABSTRACT

In this study, the process of magnetic orientation of ferromagnetic fibers used in fiber reinforced cementitious composites was investigated. The fiber's behavior during the orientation was explored in a simulation. The effect of the magnetization characteristic and fiber's orientation in the magnetic system on the resulting torque induced into the fiber is presented. Comparison of several commercially available fibers is shown.

ABSTRAKT

Tato studie se zaměřuje na zkoumání procesu magnetické orientace feromagnetických vláken používaných ve vlákny vyztužovaných cementových kompositech. Chování vláken během magnetické orientace bylo zkoumáno simulací. Vliv magnetizační charakteristiky a orientace vlákna v magnetickém systému na výsledný moment působící na vlákno je představen v této práci. Je zahrnuto porovnání několika komerčně dostupných vláken.

DECLARATION

I declare that this thesis has been composed solely by myself and that it has not been submitted, in whole or in part, in any previous application for a degree. Except where states otherwise by reference or acknowledgment, the work presented is entirely my own.

In Prague 21.05.2021 ……..

AKNOWLEDGEMENTS

I would like to thank my supervisor Ing. Karel Künzel, CSc. for his help with this thesis and insightful comments and suggestions. I would also like to thank my family and friends for their unwavering support and belief in me.

TABLE OF CONTENTS

LIST OF FIGURES

LIST OF TABLES

Chapter I: Introduction

Concrete is one of the most frequently used building materials. Although concrete itself is a brittle composite, its relatively low tensile strength and ductility can be improved by the inclusion of reinforcement. One of the commonly used materials for concrete reinforcement are fibers, which together with concrete result in a composite material with improved structural strength and durability. Improvement of concrete's ductility, decreased formation and propagation of cracks and significant improvement of energy dissipating capacity are among other important advantages of fiber-reinforced concrete (FRC). Fiber reinforcement is mainly used in shotcrete[1], but can also be used in normal concrete.

Steel fibers are the most commonly used kind of fibers due to their high tensile strength and thermal expansion similar to concrete, which eliminates large internal stresses due to differences in thermal expansion or contraction. Another quality of steel useful for this application is that the alkaline environment of concrete provides steel with corrosion protection by creating a passivating film[2].

Fibers' properties can significantly affect tensile performance of the concrete. The greatest reinforcement effect is achieved when fibers are oriented in the direction of tensile stress [1]. Many researches were conducted to determine the effects of casting method, mould shape, fibers' geometric properties, their distribution, vibration and fresh mixture's rheological properties on the final fiber orientation in cementitious composites. Although it is possible to improve mechanical properties of concrete using casting and flow, it is hard to fully control fibers' final orientation.

[1] A construction technique, where concrete or mortar, typically reinforced, is conveyed through a hose or pneumatically projected at high velocity onto a surface.

[2] A thin oxide layer formed on the steel that prevents metal atoms from dissolving.

The orientation of steel fibers in fresh concrete mixture can be changed and controlled by an external magnetic field. In a uniform magnetic field, steel fibers tend to rotate to align with the field due to the driving magnetic force. Therefore, by placing fresh concrete mixture with embedded steel fibers in homogenous magnetic field that has the same direction as the one of the tensile stress, the steel fibers can be aligned to achieve the maximum reinforcing efficiency [2]. It is important to mention that the magnetic force must be large enough to overcome viscous resistance of the concrete mixture. The final torque force effects acting on a fiber depend on the strength of magnetic field as well as fiber's magnetic properties.

Effects of fibers' non-linear behavior in the magnetic field can be studied using finite element analysis, which is the main focus of this study. Numerical analysis of the process of fiber's orientation in the magnetic field is performed in ANSYS using the finite element method (FEM) based on the fundamental Maxwell equations. Obtained characteristics are then compared to the theoretical calculations.

Chapter II: Case study

1.1 TORQUE ACTING ON A FIBER IN MAGNETIC FIELD

Fibers commonly used for the application of fiber-reinforced concrete are made of soft magnetic materials as seen from the measured magnetization characteristics (see 1.2). To further understand behavior of fibers placed in a magnetic field, we need to first overview properties of ferromagnetic materials.

On the atomic level a ferromagnetic material consists of magnetic dipoles that have permanent dipole moments [3]. One way to describe a dipole moment is an Amperian loop model (Figure 1) for each atom, where current loop is created by an electron going around proton resulting in the dipole moment $\vec{m} = I \cdot S$. The direction of the dipole moment is defined by the right-hand rule. Ferromagnetic materials then have domains (Figure 2), which are essentially groups of dipoles, where dipole moments are oriented in the same direction.

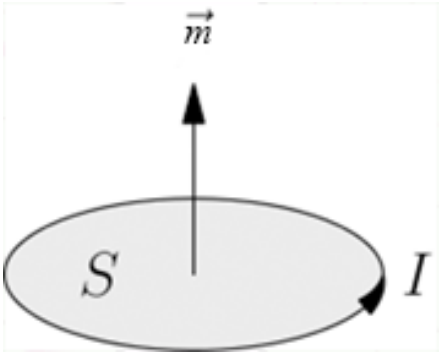

Figure 1: Amperian loop model of a dipole [4]

Exposing ferromagnetic material to an external magnetic field causes domains to align with the field, which leads to a larger magnetic field inside the material. Relation between the applied magnetic field and the one inside the material is expressed through relative permeability μ:

$$B = \mu H = \mu_0(1 + \chi_m)H, \quad (1)$$

where B is induction inside the material (T) caused by the applied magnetic field B_0 of intensity H (A/m); χ_m is magnetic susceptibility (H/m), which is the rate of magnetization increase. We can neglect vaccum permeability μ_0 equal to $4\pi \cdot 10^{-7}$H/m since magnetic susceptibility of ferromagnetic materials is much larger in comparison, ranging up to tens of thousands H/m. Then equation (1) is:

$$B = \mu H = \mu_0 \chi_m H = \chi_m B_0. \tag{2}$$

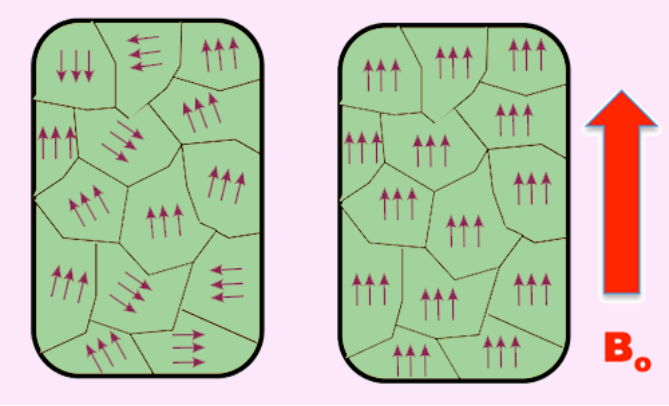

Figure 2: Domains in ferromagnetic material [5]

Relative permeability of ferromagnetic material is not constant, and it changes depending on the applied magnetic field (Figure 3). Relative permeability reaches its maximum in the linear part of magnetization characteristic and eventually decreases due to a limit, where the material reaches its maximum possible induction, called saturation induction, because all the domains are aligned with the field.

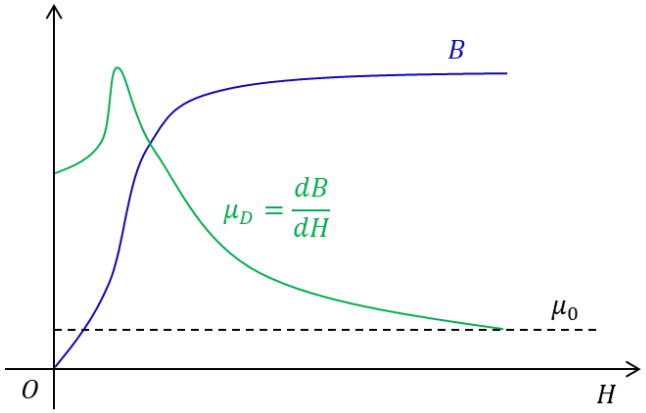

Figure 3: Magnetic permeability and induction inside a ferromagnetic material [6]

Torque acting on a fiber made of ferromagnetic material can be simplified and described for two distinctive cases: unsaturated state and saturated state. Unsaturated state is defined as a linear part of fiber's magnetization characteristic, where induction inside a fiber grows proportionally to the applied magnetic field. Magnetization characteristic can be approximated by a direct ratio:

$$B = \mu H. \tag{3}$$

Saturated state is then a part of magnetization characteristic, where the fiber has previously been magnetized and magnetic induction inside the fiber practically no longer grows, because all the domains are aligned with the field. In this case, domains create one magnetic dipole throughout the whole fiber.

We can consider that the fiber exposed to a magnetic field has a constant dipole moment in the applied field intensity in a steady state when domains are no longer changing their orientation. Then the fiber's magnetic moment can be described as a magnetic moment of a permanent magnet. A magnet can be in analogy with electrostatics represented by two opposite magnetic charges (poles) at a certain distance [8]. Magnetic moment of the fiber is then

$$\vec{m} = \frac{\vec{l} \cdot \Phi_{\mathrm{m}}}{\mu_0}, \tag{4}$$

where $\vec{m}$ is the vector of the magnetic moment (Am^2), $\vec{l}$ is the length of the fiber (m) and Φ_{m} is the magnetic charge of the dipole at the fiber's ends (Wb), which is

$$\Phi_{\mathrm{m}} = S \cdot B_n, \tag{5}$$

where S is the area of the perpendicular section of the fiber (m^2), B_n is the normal component of the magnetic induction vector on this surface (T).

With an assumption that the magnetic field $\vec{B}$ into which the fiber is inserted is homogenous and the fiber is so small that it does not affect the field, we can express torque $\vec{T}$ (Nm) acting on a fiber as:

$$\vec{T} = \vec{m} \times \vec{B}. \tag{6}$$

Torque acting on a fiber can then be described for the two states, unstaturated and saturated respectively, with all above mentioned assumptions and considerations in mind, as follows:

$$|\overrightarrow{T_{unsat}}| = |\vec{m} \times \vec{B}| = \frac{1}{2}\frac{S \cdot l \cdot \mu|\vec{B}|^2}{\mu_0} sin\, 2\alpha, \tag{7}$$

$$|\overrightarrow{T_{sat}}| = |\vec{m} \times \vec{B}| = \frac{S \cdot l \cdot f_B(|\vec{H}|\, cos\, \alpha)}{\mu_0} \cdot |\vec{B}| \cdot sin\, \alpha. \tag{8}$$

$\vec{T}$ is the vector of the torque (Nm),

$\vec{m}$ is the vector of the magnetic moment (Am^2),

$\vec{B}$ is the magnetic field induction vector (T),

α is the angle between vectors $\vec{m}$ and $\vec{B}$,

$f_B(|H|\, cos\, \alpha)$ is the value of fiber's induction in the magnetic field of intensity $\vec{H}$ (A/m) projected onto fiber's axis,

$\mu|B|$ is the linear approximation of fiber's magnetization characteristic.

We can draw following conclusions from these equations:

- unsaturated state (linear magnetization part): torque acting on a fiber is proportional to the square of the magnetic field strength; as the fiber rotates, torque reaches its maximum value at 45° angle from the direction of the magnetic field lines; if the fiber axis is perpendicular or parallel to the magnetic field lines, torque does not occur,
- saturated state (previously magnetized): induction inside the fiber practically no longer grows, the fiber then behaves like a permanent magnet; torque is proportional to the intensity of the magnetic field; as fiber rotates, torque grows as the angle

increases, and reaches its maximum value when the fiber is perpendicular to the magnetic field lines.

In reality, as the fiber rotates the transition between the unsaturated and saturated state may occur, where a fiber that was not previously magnetized and that is exposed to a sufficient magnetic field intensity, becomes magnetized and reaches its saturation induction. Equations (7) and (8) do not describe the real non-linear behavior of a ferromagnetic fiber during the orientation process, but gives a general understanding of torque acting on the fiber for two simplified states, unsaturated and saturated.

1.2 MAGNETIC PROPERTIES OF FIBERS

The materials, which fibers used in composites are made of, are mainly chosen for their mechanical properties, so that the resulting composite's tensile strength and ductility are improved. Datasheets [9-13] of commercially available fibers specify their dimensions, strength, flexibility, and corrosion resistance, but magnetic properties are not guaranteed nor specified in any way.

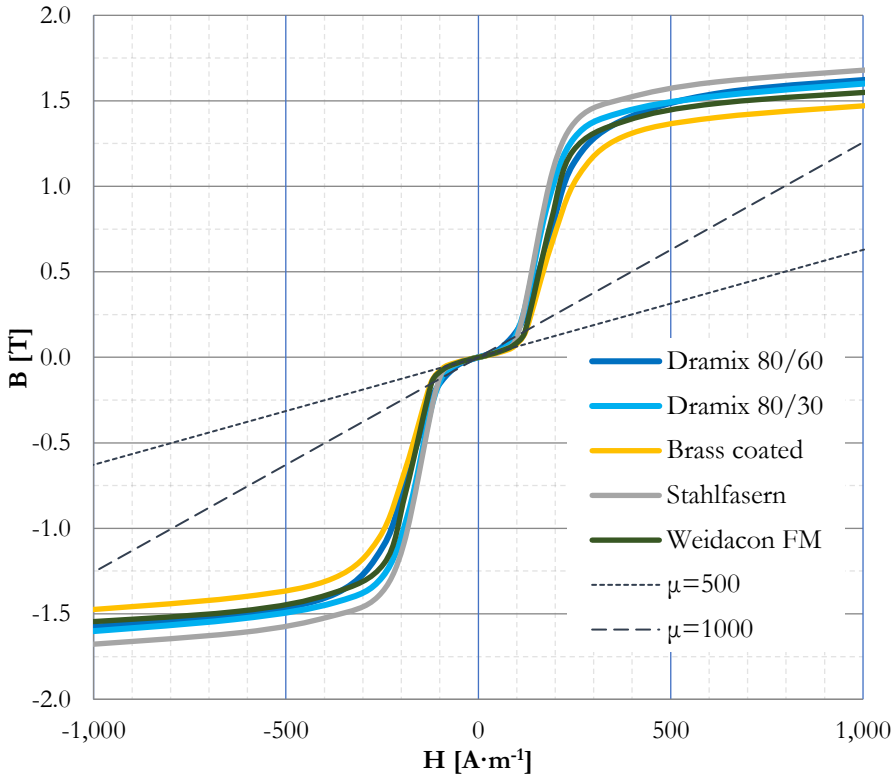

Figure 4: Initial magnetization curves of selected fibers

The measurement of selected fiber's magnetization characteristics is described in [7]. Obtained initial magnetization and hysteresis data are shown in Figure 4 and Figure 5. We can see from the graphs that the ferromagnetic fibers used in concrete composites behave similarly in a magnetic field. They have relatively low initial permeability ranging from around 500 H/m to 1000 H/m; hence, the force acting on such fibers in a weak magnetic field is not significant. Torque acting on such a fiber in this case would not be sufficient for its successful orientation. The fiber placed in a magnetic field of a sufficient intensity has a rapid increase of the magnetic induction to values comparable to "magnetically high-quality material".

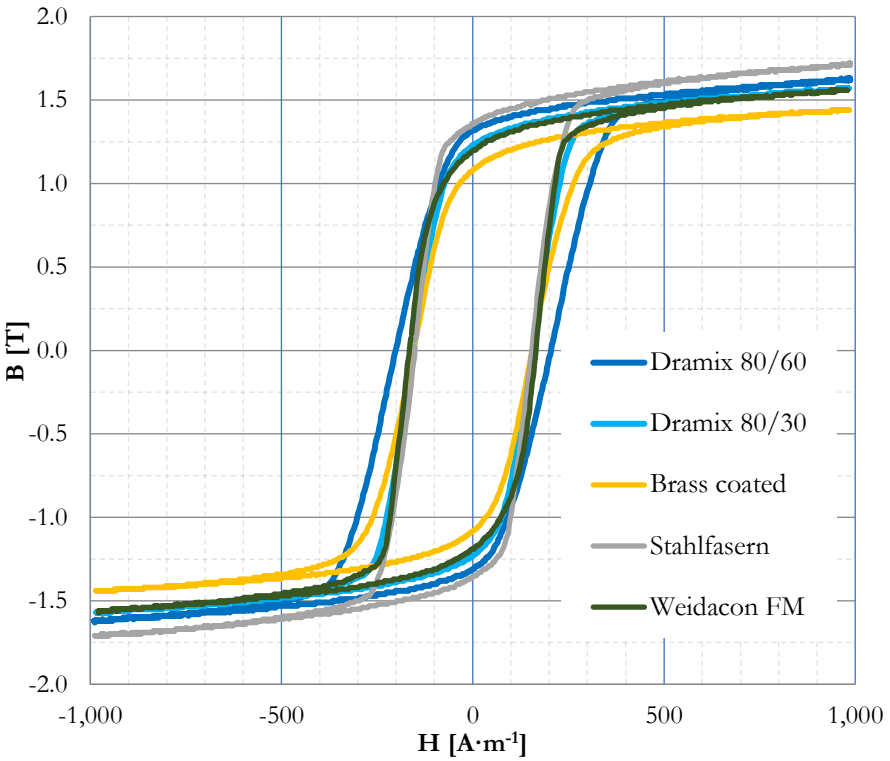

Figure 5: Magnetic hysteresis curves of selected fibers

Different fibers' hysteresis curves are very similar. The difference in width and slope of the curve and in value of remanent induction is not large and should not cause significant differences in the induced torque during magnetic orientation. Fibers' hysteresis curves are relatively wide, meaning higher hysteresis loss of the material. However, this does not affect the fiber's final orientation, but this quality of the fiber's material can be used for a non-destructive testing of the fiber-reinforced concrete based on a measurement of a quality factor of a coil [7]. In other words,

the higher the number of fibers oriented in the direction of the field which the composite is exposed to, the higher the losses that affect the measuring coil's magnetic circuit properties.

Combined magnetization characteristics for the individual fibers are shown in Figure 6. Saturation induction of the individual fibers is given in Table 1.

	Saturation induction (T)
Dramix 80/60	1.60
Dramix 80/30	1.53
Weidacon FM	1.51
Brass coated	1.42
Stahlfasern	1.72

Table 1: Saturation induction of selected fibers

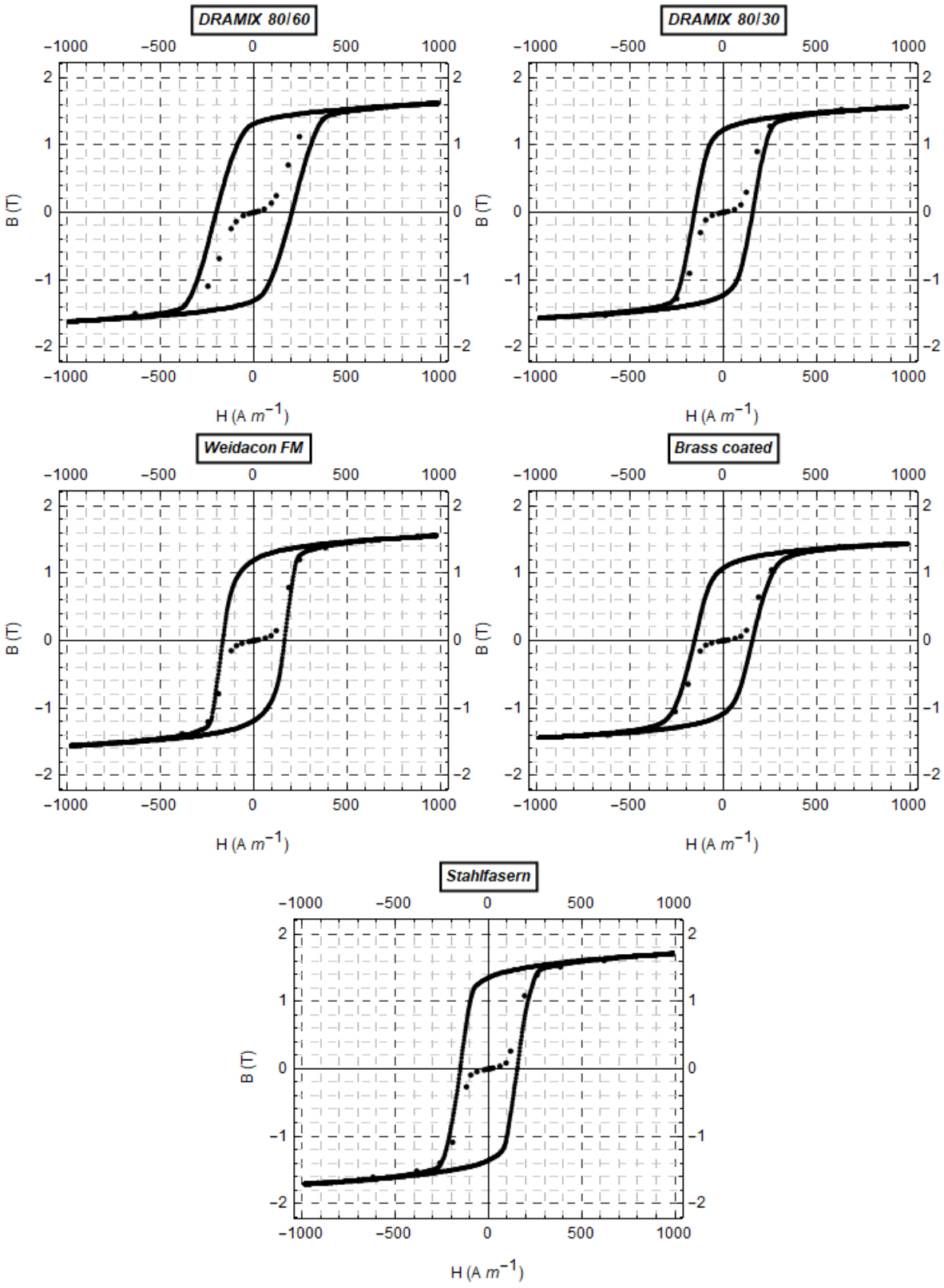

Figure 6: Magnetization characteristics of selected fibers

Chapter III: Modeling of experimental setup

2.1 MODEL OF THE SYSTEM

Fibers' behavior in the magnetic field was simulated in ANSYS (ANSYS Workbench, 2020 R1, ANSYS Inc.). A model of the experimental setup, with dimensions and parameters described below, was created for simulating of torque acting on a fiber in a magnetic field. This model consists of two air-cored coils supplied with 24 A current, which creates a homogenous DC magnetic field of approximately 25 mT in the center of the system where the fiber is being placed (Figure 7). Each coil has the following parameters:

$$L = 30.5\ mH,$$
$$R = 0.95\ Ohm,$$
$$n = 13,$$
$$d = 2.6\ mm,$$

where L and R are the inductance and resistance of each coil respectively, n is the number of layers and d is the gauge of the wire used to construct this coil. The estimated number of turns is 208, which is used as one of the input parameters for the simulation along with the supplied current and the conducting area of the coil. The number of turns N was calculated as follows:

$$N = n \cdot \frac{w}{d \cdot k},$$

where w is the width of the coil and k is the winding distribution coefficient equal to 1.1.

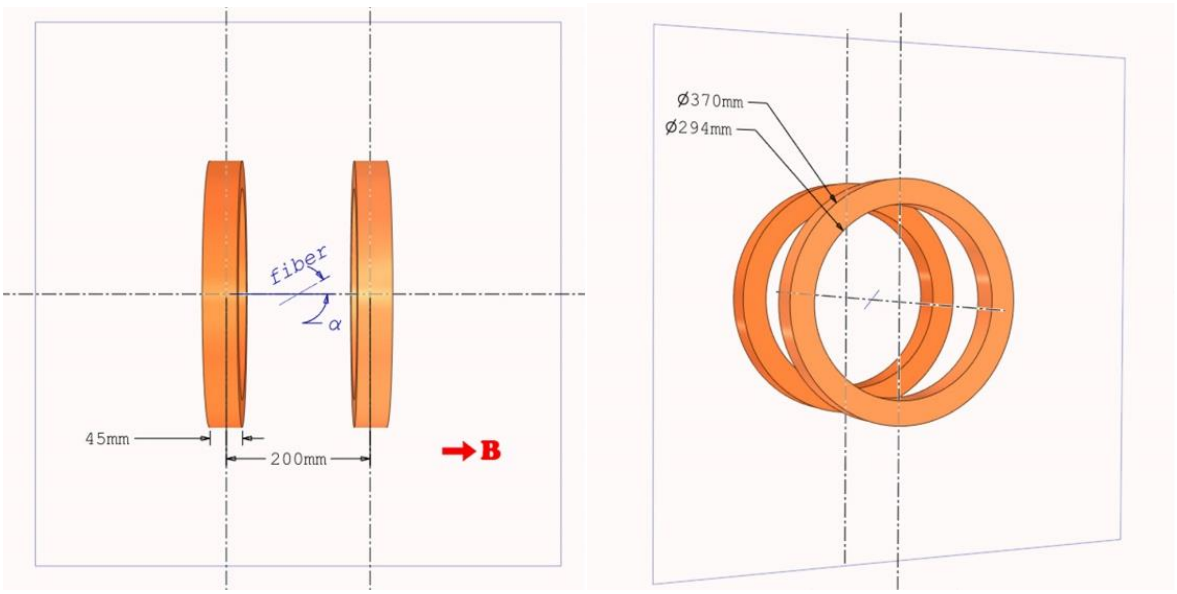

Figure 7: Experimental setup model drawing

The measured fiber is always placed in the center of the system at the angle α from the direction of the external magnetic field B. Models of the fibers with dimensions given in Table 2 and magnetization characteristics shown in Figure 6 were created. Fiber's dimensions were found in manufacturers datasheets [9-13].

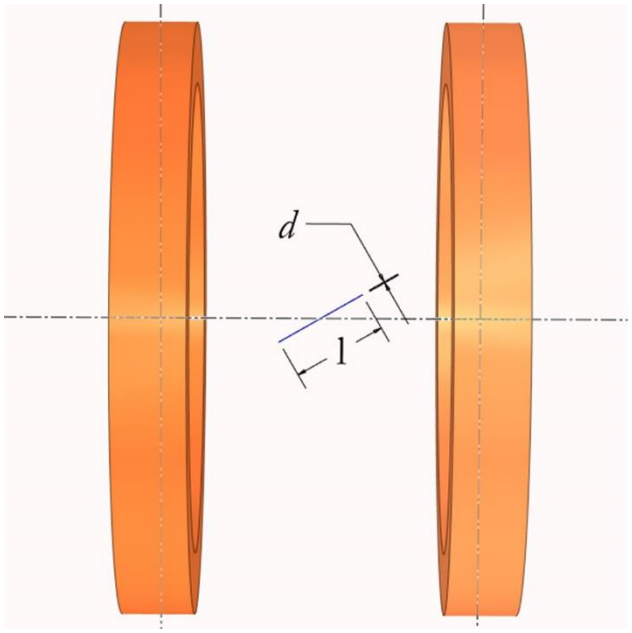

Figure 8: Fiber dimensions

	r (mm)	l (mm)
Dramix 80/60	0.4	60
Dramix 80/30	0.2	30
Weidacon FM	0.075	6
Brass coated	0.144	12.5
Stahlfasern	0.09	13

Table 2: Fiber dimensions

Since the real fibers have complex shapes – hooked (Dramix 80/60, Dramix 80/30) or wavy (Weidacon FM, Brass coated, Stahlfasern) (Figure 10) – their models are approximated by a straight cylinder of length l (mm) and radius r (mm).

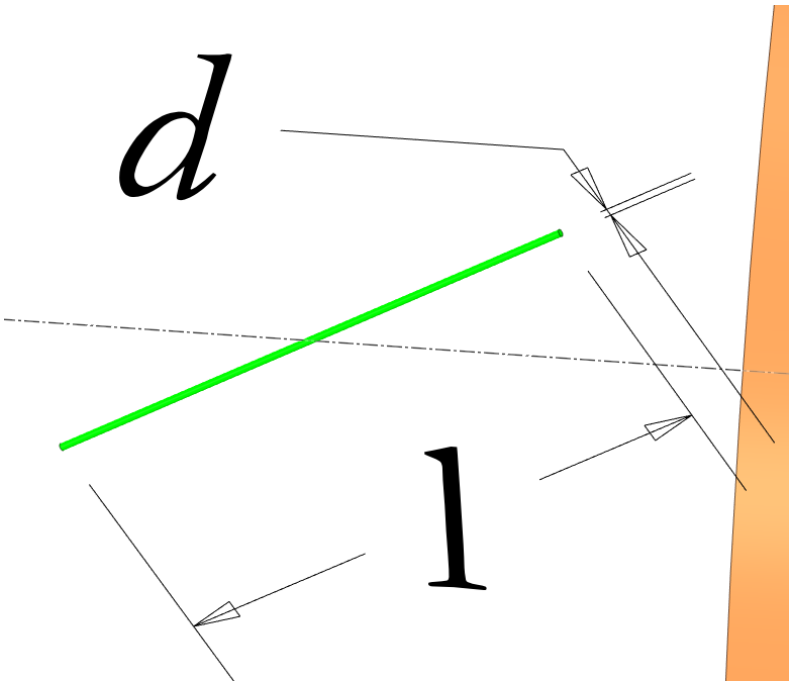

Figure 9: Model of a fiber

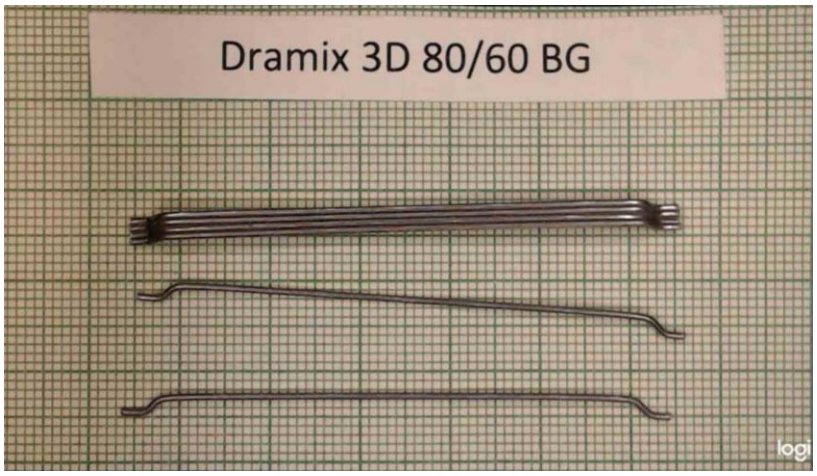
Dramix 3D 80/60 BG


Dramix 3D 80/30 GGP

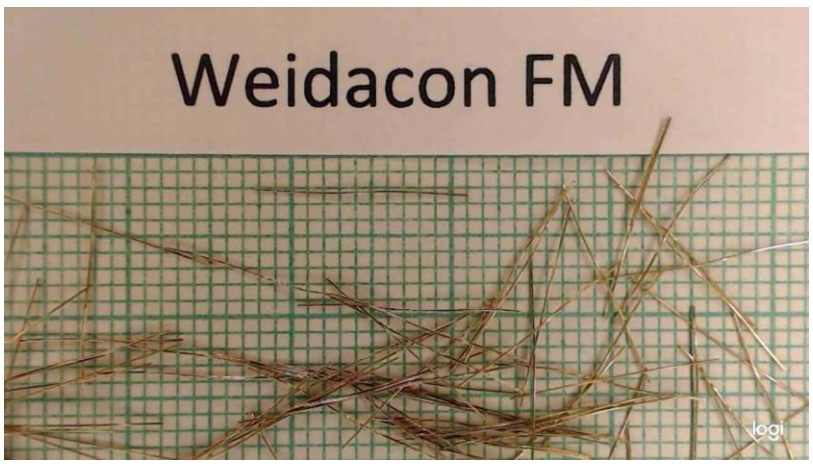
Weidacon FM

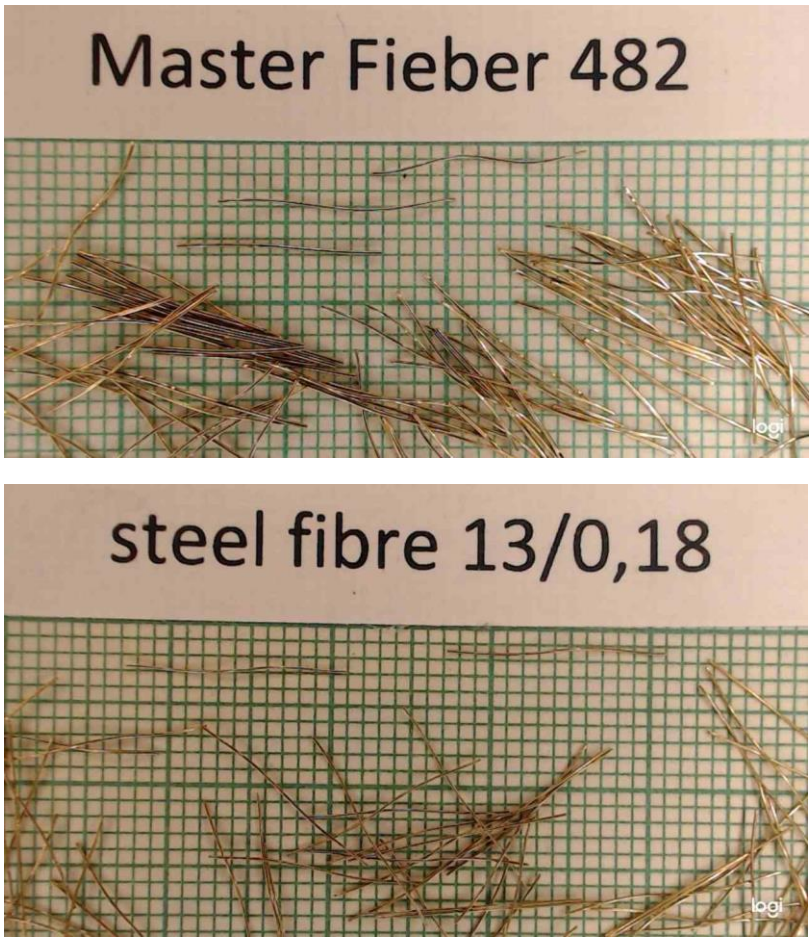

Figure 10: Fiber samples

2.2 MATHEMATICAL MODEL OF THE MAGNETIC HYSTERESIS CURVE

Magnetic hysteresis curve, or B-H curve, describes the non-linear behavior of magnetization that the ferromagnetic material obtains when exposed to a magnetic field. Its smoothness can greatly affect a simulation. Measurement data require pre-processing for a successful simulation. Each set of measured hysteresis curves contains 2000 samples measured with a time step of 10 μs. Raw measurement data for the fiber Dramix 80/60 is shown in Figure 11. Measured values are more sparsely distributed for a steeper part of the characteristic, where $\frac{dB}{dH}$ is quite large. Part of the characteristic, where the fiber transitions into a saturated state, contains ripples that may cause

numerical instabilities that result in longer computation times or even a lack of convergence. A mathematical model of magnetic hysteresis needs to be created.

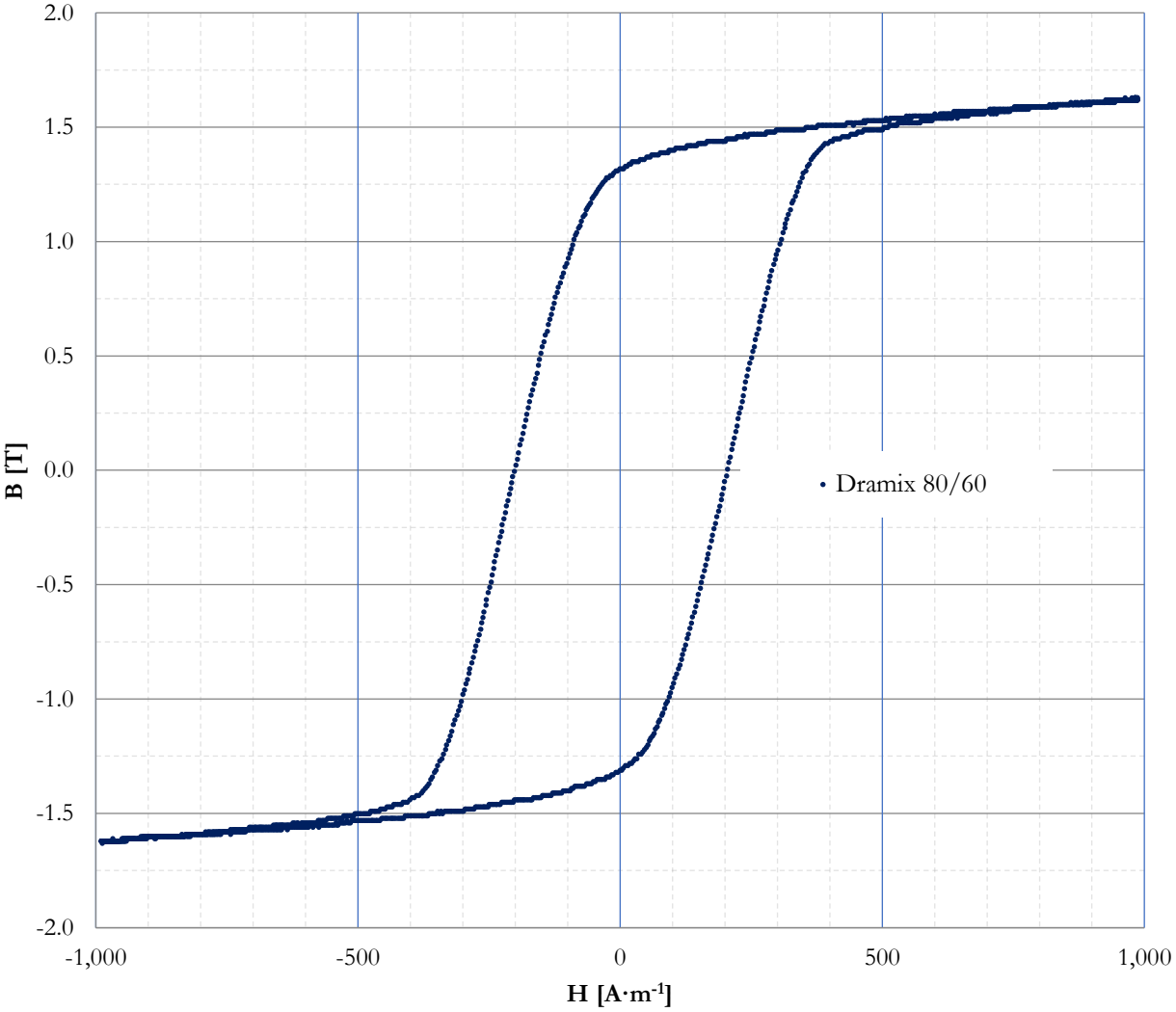

Figure 11: Raw magnetic hysteresis measurement data

A number of mathematical approaches had been used to model the behavior of ferromagnetic materials. One of the first models of magnetic hysteresis curve is the Langevin function (1905), which describes the saturation effect for the anhysteretic curve. This function then evolved into many different forms of various levels of complexity to best describe the non-linear behavior of ferromagnetic materials.

Since in our case a magnetized fiber is being placed in a DC magnetic field, we essentially only need the upper part of the hysteresis loop in the I. quadrant (where B and H are positive), if we consider that the fiber is magnetized in the direction of $\vec{m}$ as shown in Figure 12. Fiber's induction will be larger at a smaller deviation from magnetic field lines, and it will decrease if the fiber is perpendicular to magnetic field lines, experiencing demagnetizing effect due to some part of domains changing their orientation in the direction of the field.

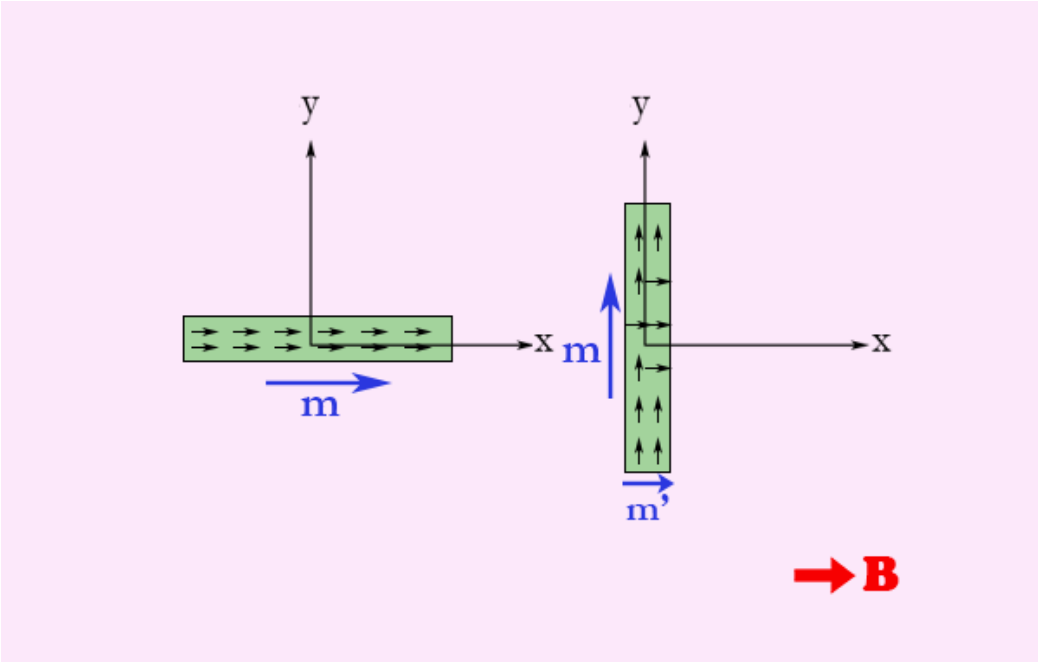

Figure 12: Magnetized fiber's domains at 0° and 90 ° deviation

This work focuses on a general behavior of fibers in the magnetic field, therefore a complex precise model of fibers is not needed. Measured data was approximated with a simple $ArcTan$ function using the least squares method:

$$f(x) = a \cdot ArcTan\big(b \cdot (x - c)\big) + d,$$

where x represents magnetic field intensity H and $f(x)$ represents fiber's magnetic induction B. Constants a, b, c, d for individual fibers are given in the table below:

	a	b	c	d
Dramix 80/60	1.090	0.012	-203.150	-0.035
Dramix 80/30	1.025	0.018	-155.364	-0.027
Weidacon FM	1.008	0.021	-163.863	-0.032
Brass coated	0.956	0.014	-156.591	-0.025
Stahlfasern	1.105	0.021	-153.742	-0.028

Table 3: Hysteresis curve model constants

Fitted hysteresis models (Red) for individual fibers are shown in Figure 13. The models differ slightly from the fibers' hysteresis curves, but these models are sufficient for general understanding of the fiber's behavior in the magnetic field. Note the differences in the saturation induction of the model and measured data. This will be considered in the simulation results evaluation described in the next chapter as it may cause a difference in a magnetized and non-magnetized fiber' behavior in a saturated state.

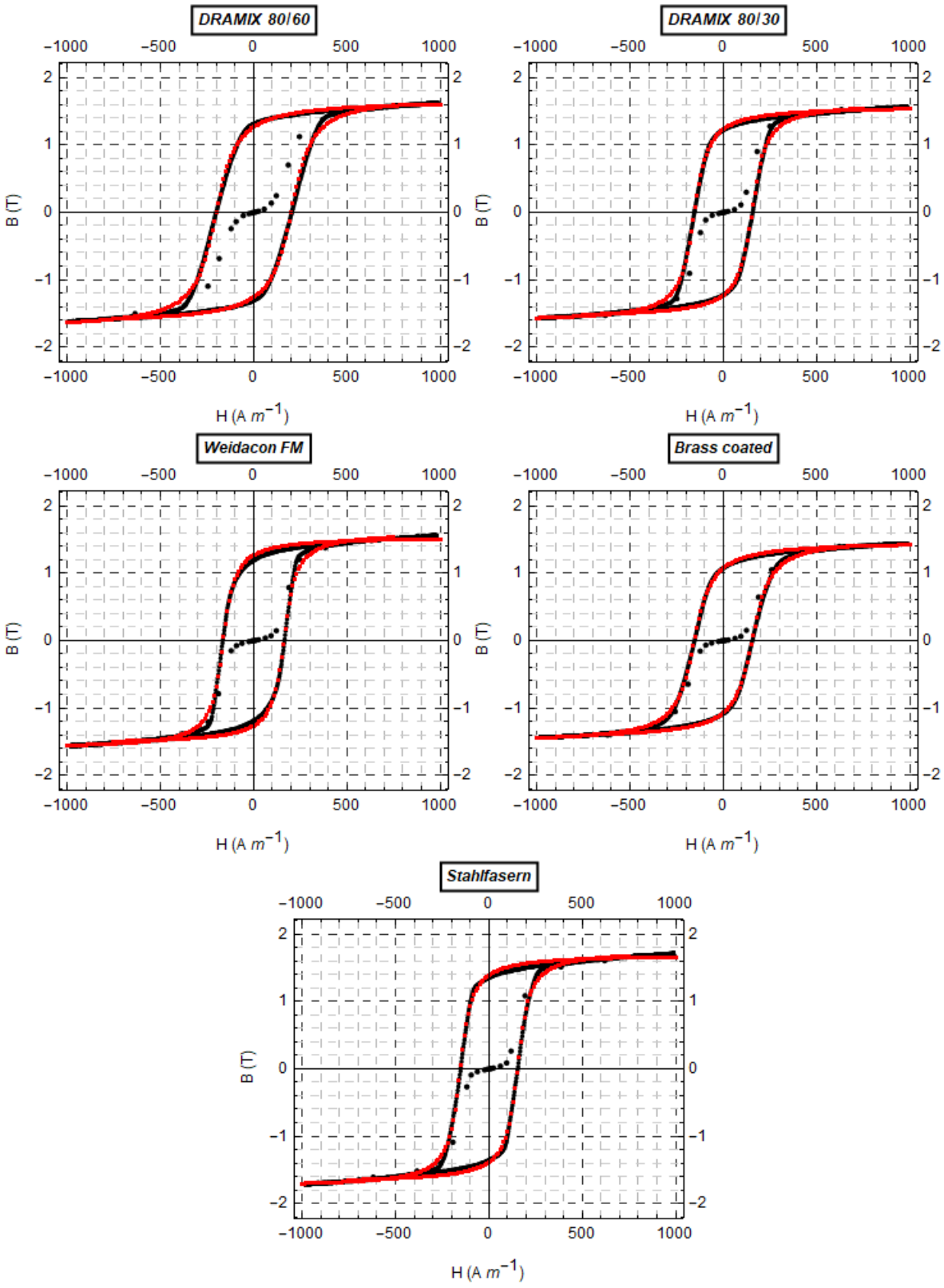

Figure 13: Hysteresis curve models

2.3 SIMULATION MEASUREMENT SETUP

The analyzed fiber is rotating in a homogenous magnetic field (Figure 14) of predefined strength. The magnetic field strength is controlled by setting different values of current going through the coils (Figure 15). The external field was measured in the center of the system without a fiber. Values of currents corresponding to the desired external fields were chosen experimentally.

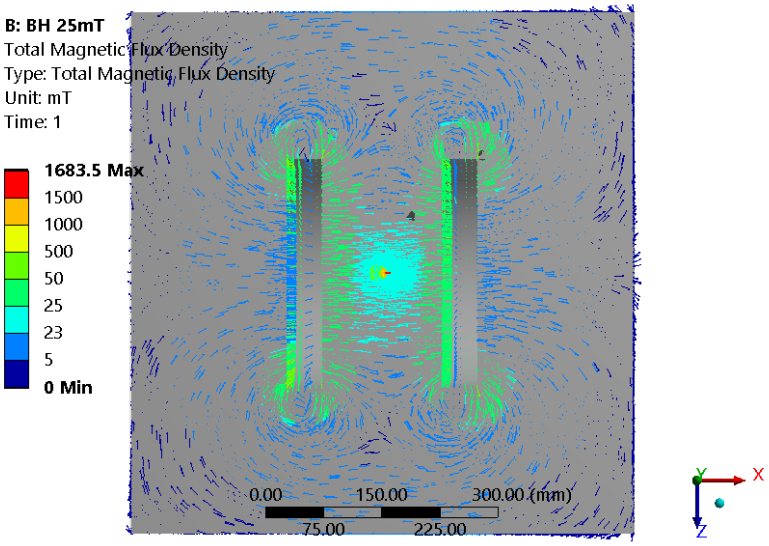

Figure 14: Magnetic field inside the system

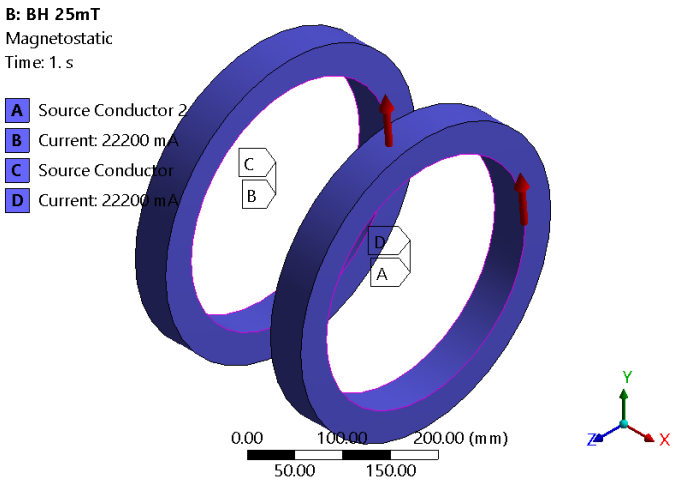

Figure 15: Direction of the current going through the coils

Settings of the current corresponding to the measurements described in the next chapter are shown below:

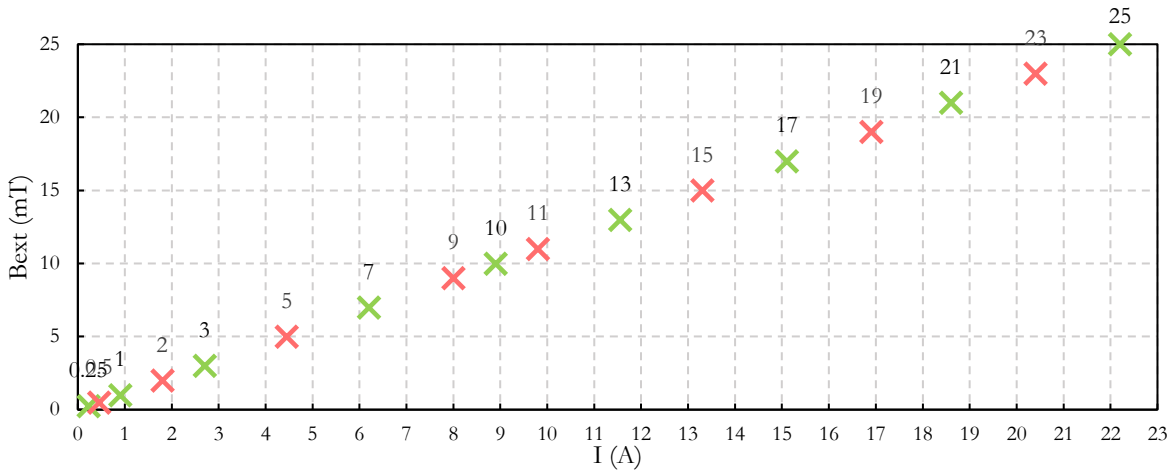

Figure 16: Simulation settings: current going through the coils

B_{ext} (mT)	0.25	0.5	1	2	3	5	7	9	10	11	13	15	17	19	21	23	25
I (A)	22.2	20.4	18.6	16.9	15.1	13.3	11.55	9.8	8.9	8	6.2	4.45	2.7	1.8	0.9	0.45	0.225

Table 4: Simulation settings: current going through the coils

Fiber's coordinate system is shown in Figure 17. The fiber is rotating about its Z axis from 90º to 0º deviation from the external field lines (the direction of system's X axis). The main measured parameters are fiber's total induction (flux density) and torque acting on it. Both flux density and torque probes are placed in the fiber coordinate system. Torque is measured in the direction of fiber's Z axis. In this setup as the fiber is trying to align with the field, torque is acting on a fiber in the direction of -Z fiber's axis. The values of torque displayed in the graphs in the next chapter are absolute values of the measured torque.

Each individual fiber has two geometrically identical models (Table 2) but two different magnetization characteristics: a magnetized and a non-magnetized state (Figure 13). A mathematical model of the hysteresis curve was used for the magnetized state. It is also worth mentioning that every measurement point (for example 10 mT, 70º deviation) does not consider the fiber's previous state (for example 10 mT, 75º deviation if we consider that the fiber is rotating

from 90º to 0º). The fiber's initial state is at $H = 0$ A/m on the magnetization characteristic at every measurement point: the non-magnetized fiber's induction is zero and the magnetized one has the value of remanent induction.

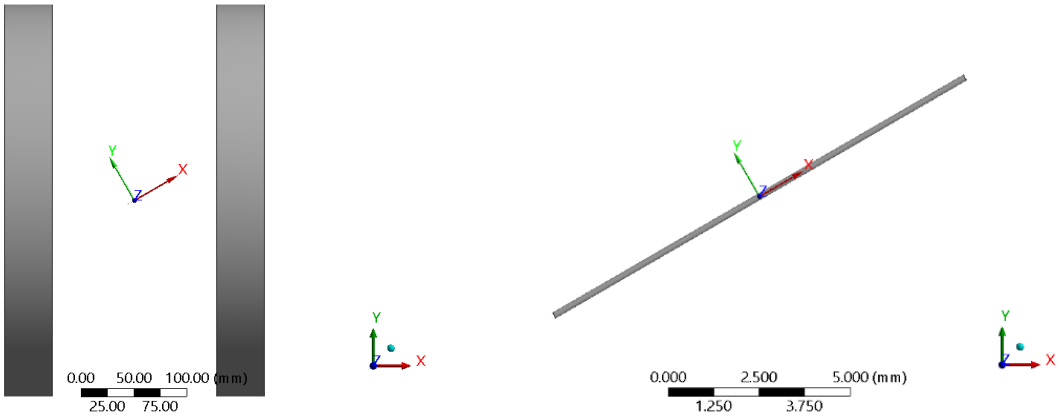

Figure 17: Fiber's coordinate system: 30º deviation

Chapter IV: Simulation results

3.1 FIBER'S BEHAVIOR IN MAGNETIC FIELD

From the theoretical background described in 1.1 we know that torque acting on a fiber in a magnetic field is dependent on the fiber's dimensions, magnetization characteristic, external field magnitude and fiber's orientation in relation to the field lines. Since fiber's dimensions are a constant, and magnetization characteristics of fibers used for the application of fiber-reinforced concrete are very similar, a detailed overview of fiber's behavior in the magnetic field was done for one selected fiber, Dramix 80/60. Simulated torque characteristics of the rest of the selected fibers can be found in 3.2 and Appendix.

Several points on the magnetization characteristic were chosen (Figure 18): a point in the linear part of magnetization characteristic, which corresponds to the unsaturated state (0.25 mT), a point where the fiber is saturated (1 mT) and one in the transition between the two (0.5 mT).

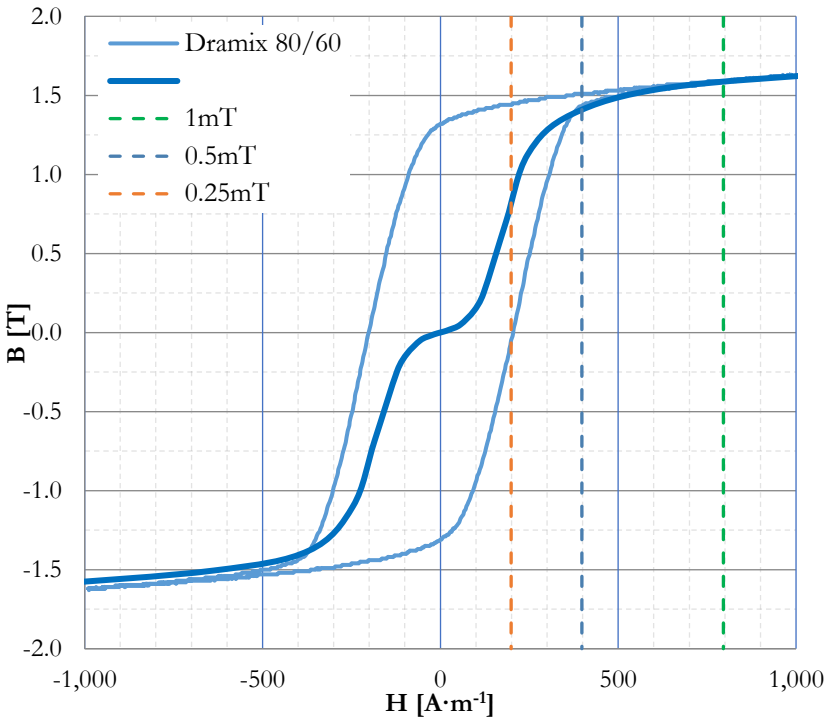

Figure 18: External field values

In theory, any field above 1 mT should result in a saturated fiber, considering the fiber is being magnetized along its axis. In our case as the fiber that has previously been magnetized is rotating, it is experiencing a demagnetizing effect (Figure 12) when placed perpendicular to the field lines. Then the induction inside the fiber will be lower than seen on the magnetization characteristic. This effect was captured in the simulation for the fiber Stahlfasern in the external field of 25 mT (Figure 19). This fiber's remanent induction is about 1.4 T, but as seen from Figure 19 fiber's induction in the perpendicular position drops to 0.3 T. As the fiber rotates towards the field lines, it quickly becomes magnetized and is fully and uniformly magnetized at 83-85º deviation, which corresponds to a maximum torque value seen in the measured data (Figure 21, 25 mT, Magnetized).

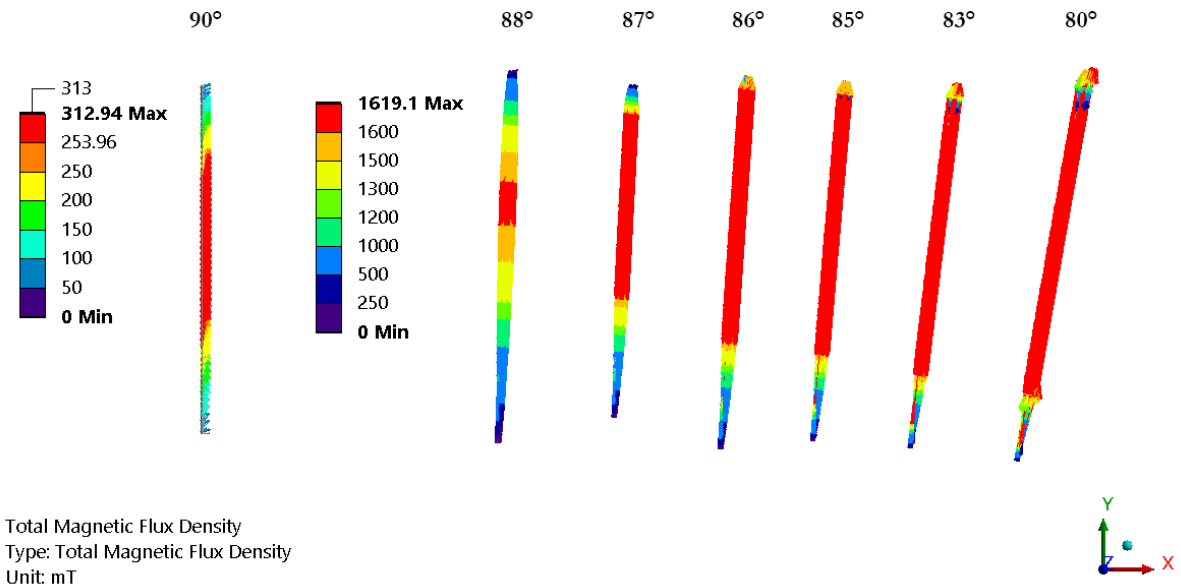

Figure 19: Demagnetization effect at 90º deviation

Induction of the fiber will increase as the fiber rotates towards the position parallel to the direction of the field until it reaches saturation (if exposed to a magnetic field of sufficient strength); this applies to both non-magnetized and magnetized fiber's initial state.

Figure 20 - Figure 22 show the simulated dependency of the torque acting on a fiber in relation to the angle from the field lines. Note the difference in the torque axis scale for individual plots. Torque acting on the fiber is following the assumptions given in 1.1.

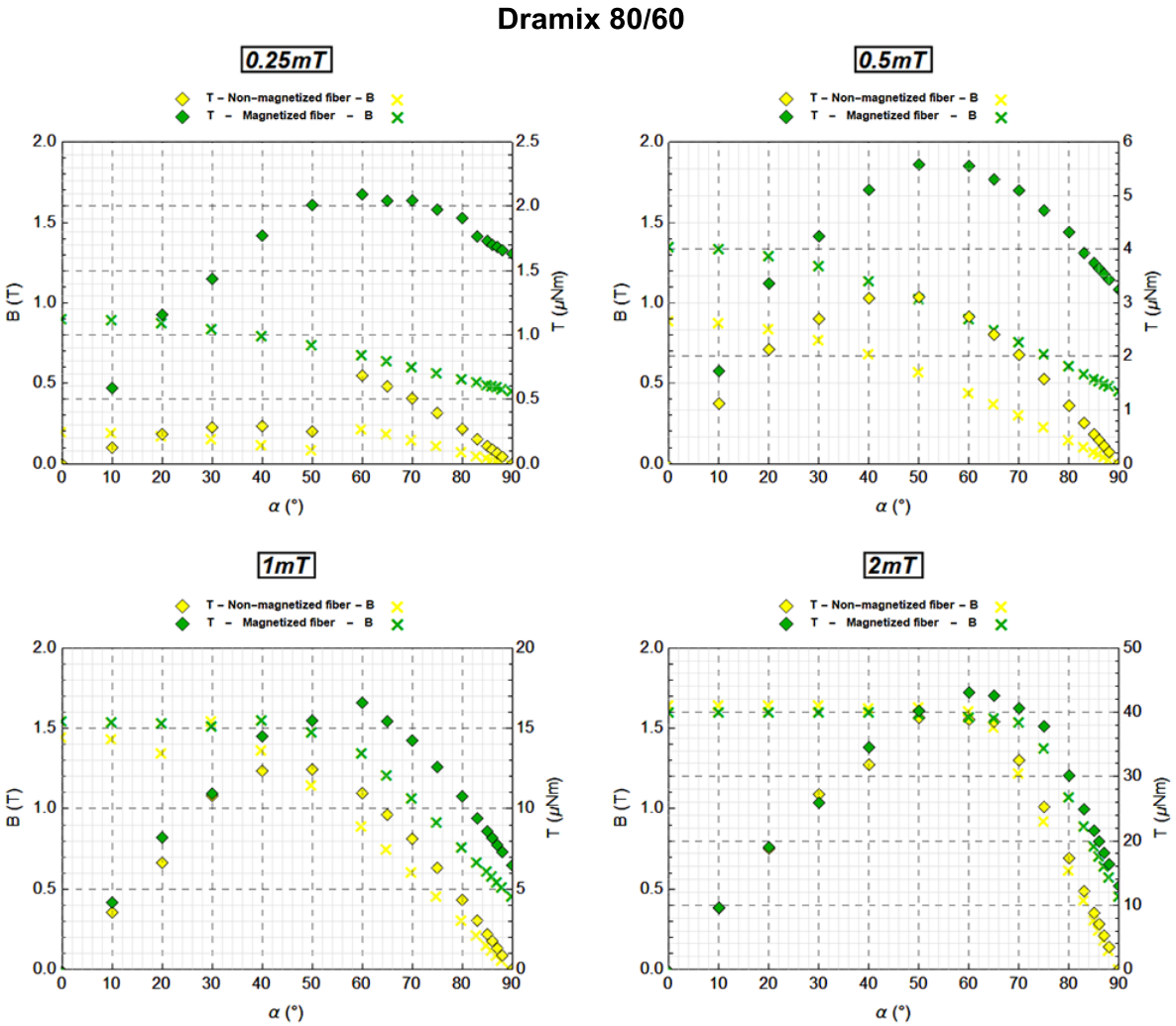

Figure 20: Torque and fiber's induction - transition into a saturated state

Let us consider that the fiber is rotating from 90° to 0° deviation from the field lines. Saturation induction of the analyzed fiber, Dramix 80/60, is about 1.6 T. As seen in Figure 20, a non-magnetized fiber's induction in the field 0.5 mT and 1 mT is in the linear part of the magnetization characteristic during the whole rotation process. A non-magnetized fiber's torque reaches its maximum at a 45° deviation. An external field of 0.25 mT is not sufficient to magnetize this fiber; fiber's induction increases up to about 0.25 T, which is approximately the beginning of the linear magnetization part, and then the fiber returns to a non-magnetized state. The external field must be large enough to overcome initial magnetization, otherwise the torque acting on the fiber is not significant. Transition between the unsaturated and saturated state occurs at an external field of 1 mT.

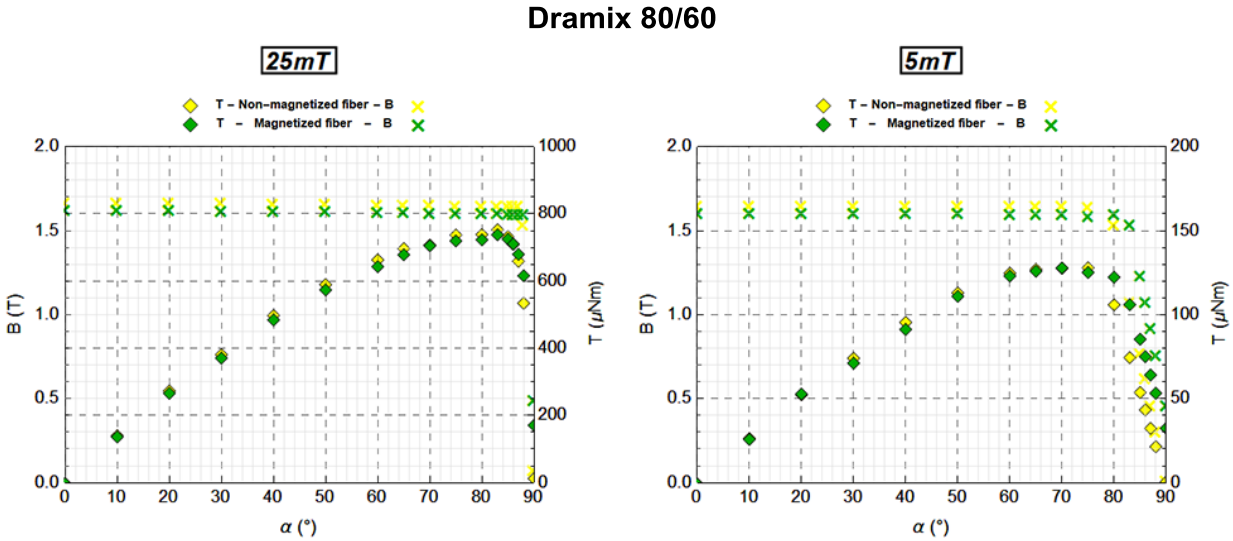

Figure 21: Torque and fiber's induction - saturated state

Comparison of fiber's torque for different external field values is shown in Figure 22. Considering again that the fiber is rotating from 90º to 0º deviation from the field lines, it can be seen that the fiber becomes magnetized faster with an increasing external field (Figure 21). This then reflects into increasing torque values. The difference between the magnetized and non-magnetized fiber's torque starts occurring at the external field of around 21 mT. The difference increases as the field decreases. This difference is dependent on how much slower the non-magnetized fiber becomes saturated in comparison to the magnetized fiber (Figure 20, Figure 21).

The difference in magnitude of magnetized and non-magnetized fiber's torque at larger field values is caused by the difference in mathematical model of the hysteresis and the initial magnetization curve (Figure 13), resulting in a slightly different saturation induction.

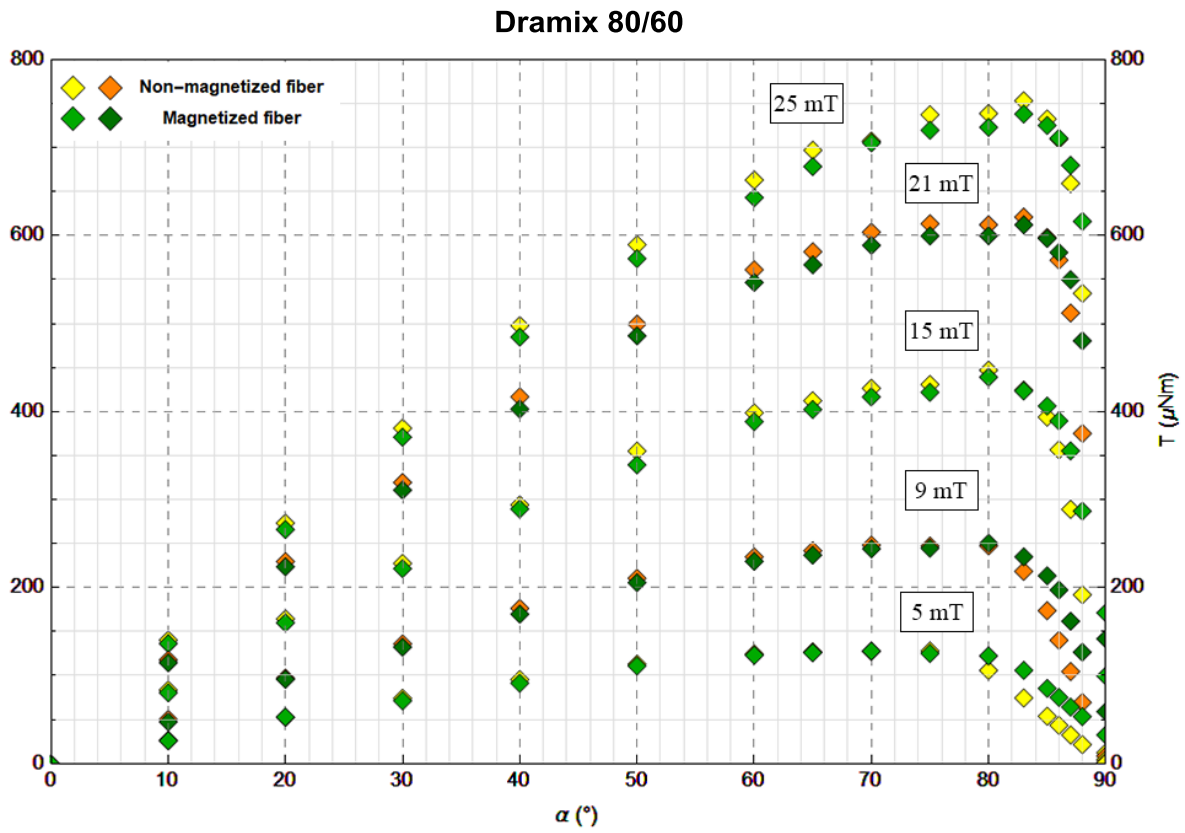

Figure 22: Torque acting on a fiber in a saturated state

3.1 CALCULATED TORQUE FOR IDEALIZED STATES

Simulated behavior of the fiber in a range of external fields gives us an overview of when the fiber's torque can be calculated as a saturated fiber's torque (1.1) defined as:

$$T_{sat} = \frac{S \cdot l \cdot B_{sat}}{\mu_0} \cdot B \cdot sin\,\alpha. \tag{9}$$

This equation should give more accurate results for larger values of external field, where the fiber reaches saturated state the fastest. As seen from Figure 21, a rotating fiber in an external field of 5 mT reaches saturation at 80° deviation. Comparison of a calculated maximum theoretical torque and simulated torque acting on a fiber for different values of external field is shown in Figure 23. Torque calculation for the saturated state gives results of a certain level of accuracy. It does not reflect a real non-linear behavior of the fiber but gives a general understanding of the

fiber's torque in a certain external field. As seen from this comparison, calculation of torque for a saturated fiber is usable down to about 3 mT - 5 mT external field. Values of saturation induction for individual fibers and their dimensions are given in Table 1 and Table 2.

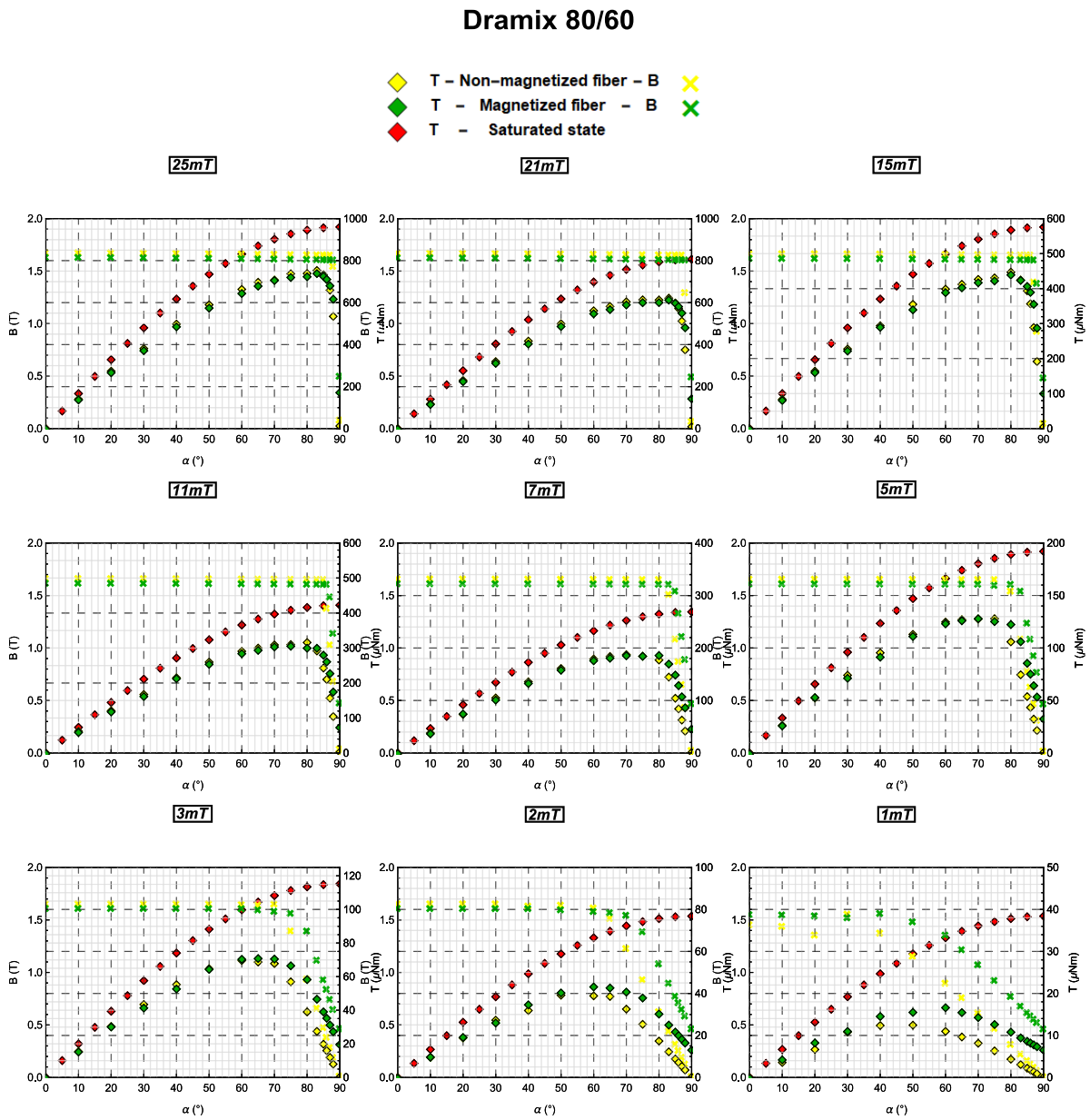

Figure 23: Comparison of simulated and calculated torque for a saturated state

For smaller external fields we need to consider that the fiber may not reach saturated state and the fiber's induction will stay in the linear part of the magnetization characteristic.

$$T_{unsat} = \frac{1}{2} \cdot \frac{S \cdot l \cdot \mu B^2}{\mu_0} sin\, 2\alpha, \tag{10}$$

The value of μ is estimated from the beginning of magnetization characteristic as shown below:

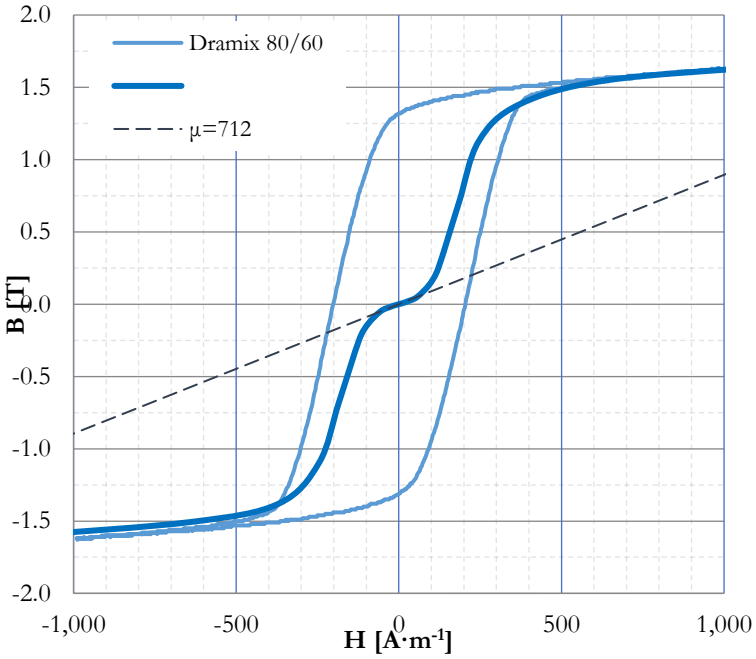

Figure 24: Initial permeability for unsaturated torque calculation

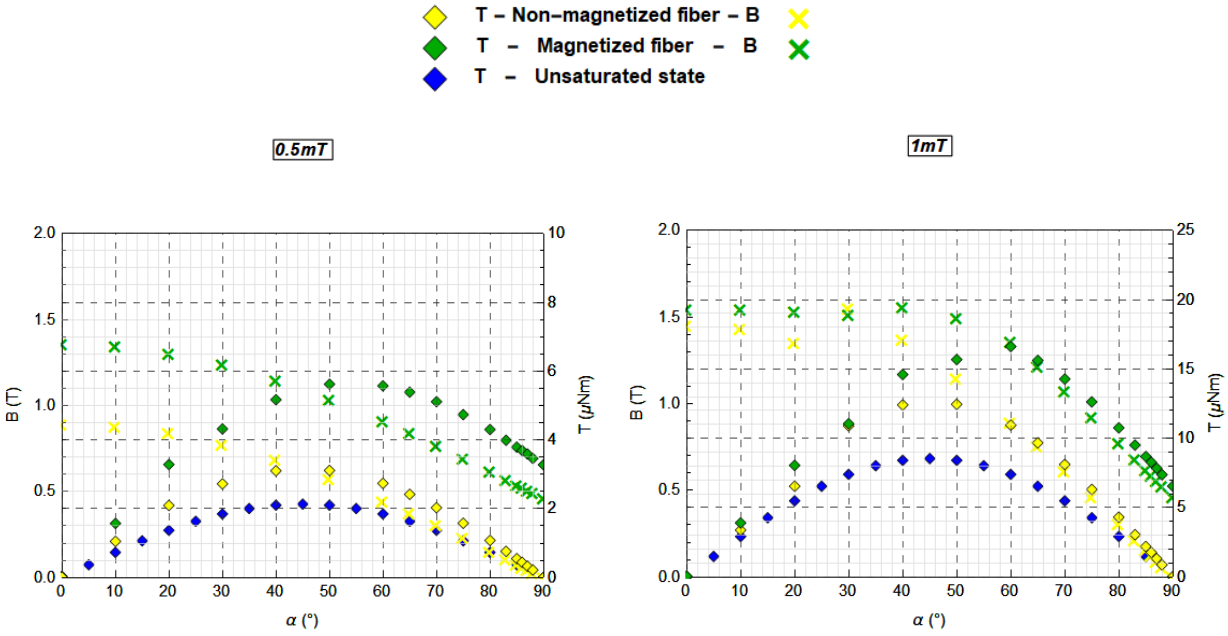

Figure 25: Comparison of simulated and calculated torque for unsaturated state

3.2 COMPARISON OF SELECTED FIBERS

Comparison of selected fibers' behavior in magnetic field was done for several external field values:

- saturated state: 5 mT, 10 mT, 25 mT
- transition: 1 mT
- unsaturated state: 0.25 mT, 0.5 mT

Plots of results for all above mentioned states and all selected fibers can be found in Appendix. Similarities in torque characteristics of different fibers due to similar magnetization characteristics are visible from the below plots:

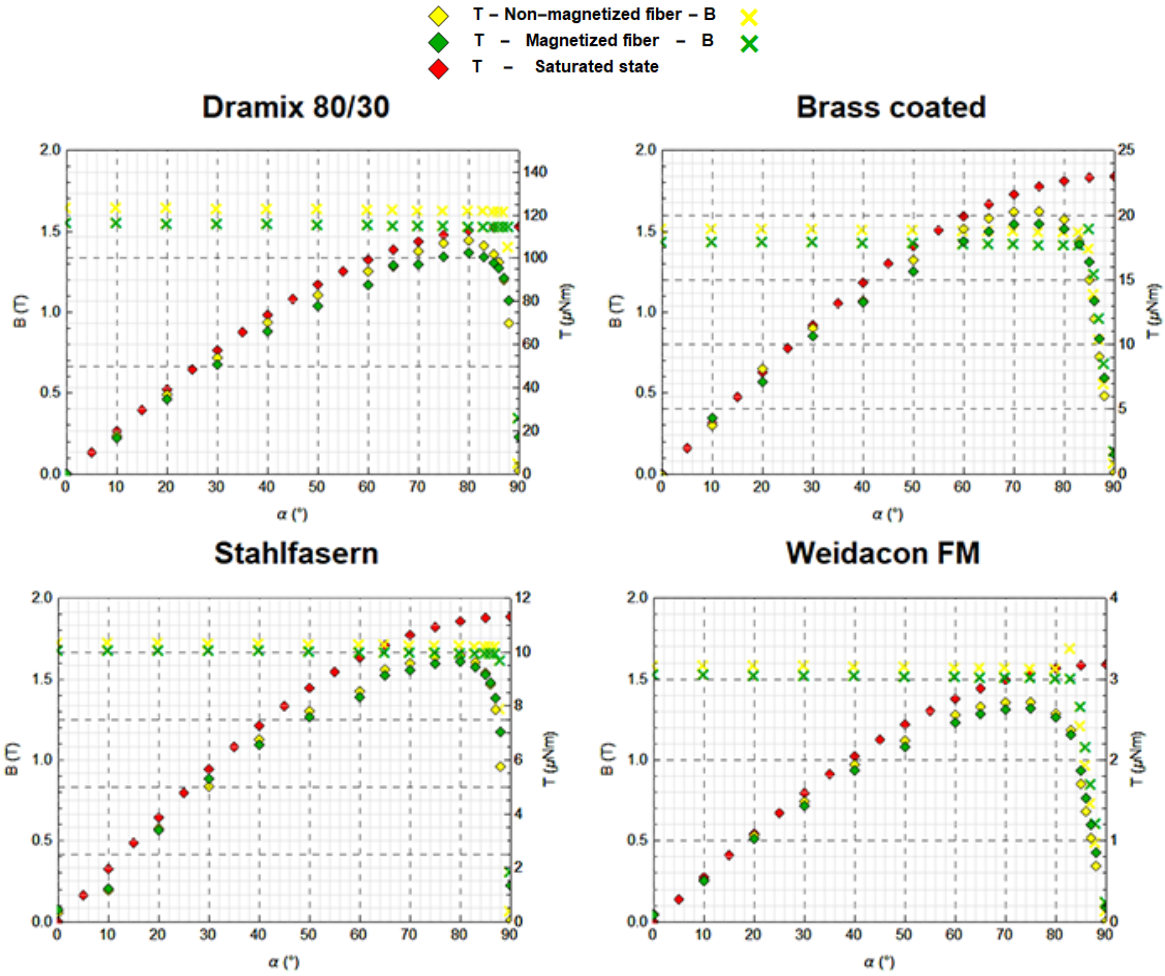

Figure 26: Torque of selected fibers - 25 mT

It can be seen from Figure 27 that the calculation of torque acting on a saturated fiber gives better accuracy at lower external fields for fibers with sharper, meaning a steeper transition into a saturated state, and narrower magnetization characteristics (Figure 6), Dramix 80/30 and Stahlfasern.

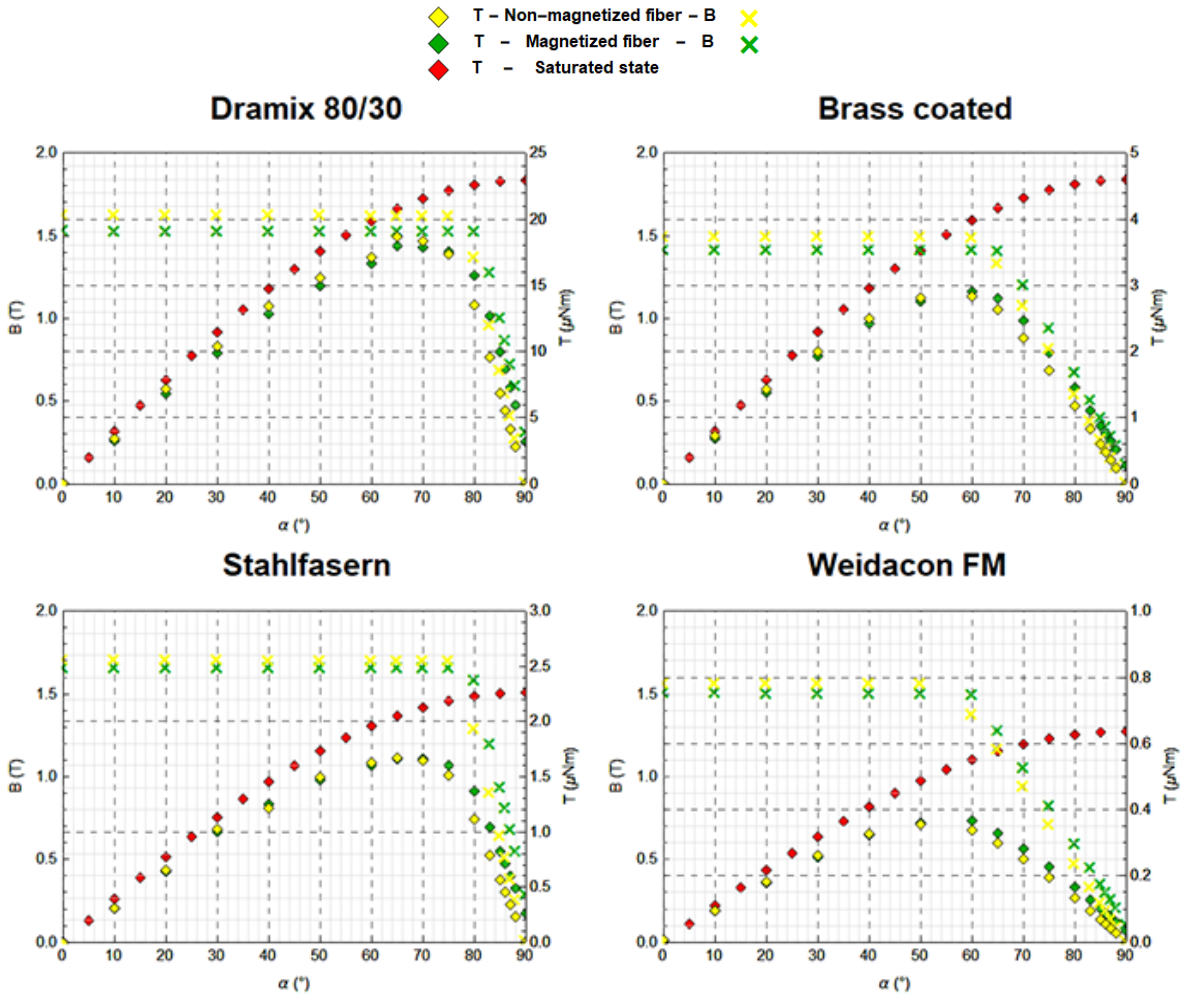

Figure 27: Torque of selected fibers - 5 mT

Values of the maximum theoretical torque T_{sat} induced into a saturated fiber in comparison with the maximum values measured within the simulations T_{sim} are presented in Table 5. The maximum theoretical torque is calculated for a saturated fiber placed perpendicular to the external field direction. Equation (9) then simplifies to

$$T_{sat} = \frac{S \cdot l \cdot B_{sat}}{\mu_0} \cdot B. \tag{11}$$

Values of saturation induction for individual fibers and their dimensions are given in Table 1 and Table 2. Example of maximum theoretical torque calculation for a saturated fiber Weidacon FM in the external field of 10 mT:

$$T_{sat} = \frac{\pi r^2 \cdot l \cdot B_{sat}}{\mu_0} \cdot B = \frac{\pi \cdot (0.075 \cdot 10^{-3})^2 \cdot 6 \cdot 10^{-3} \cdot 1.51}{4\pi \cdot 10^{-7}} \cdot 10 \cdot 10^{-3} = 1.27\ \mu Nm$$

T(μNm) / **Fiber**	25 mT		10 mT		5mT	
	$\mathbf{T_{sim}}$	$\mathbf{T_{sat}}$	$\mathbf{T_{sim}}$	$\mathbf{T_{sat}}$	$\mathbf{T_{sim}}$	$\mathbf{T_{sat}}$
Dramix 80/60	738	960	281	384	127	192
Dramix 80/30	102	114	38	45.9	18	23
Brass coated	19.3	23	7	9.2	2.9	4.6
Stahlfasern	9.88	11.32	3.65	4.53	1.66	2.26
Weidacon FM	2.64	3.18	0.93	1.27	0.37	0.64

Table 5: Comparison of simulated and saturated fiber's torque maximum

Comparison of simulated and calculated torque for unsaturated state is shown in Figure 28 and Figure 29. Torque is calculated using equation (10). Estimated values of initial permeability for individual fibers needed for the theoretical torque calculation for unsaturated state are given in the table below:

	μ (H/m)
Dramix 80/60	712
Dramix 80/30	531
Brass coated	379
Stahlfasern	515
Weidacon FM	304

Table 6: Estimated initial permeability of selected fibers

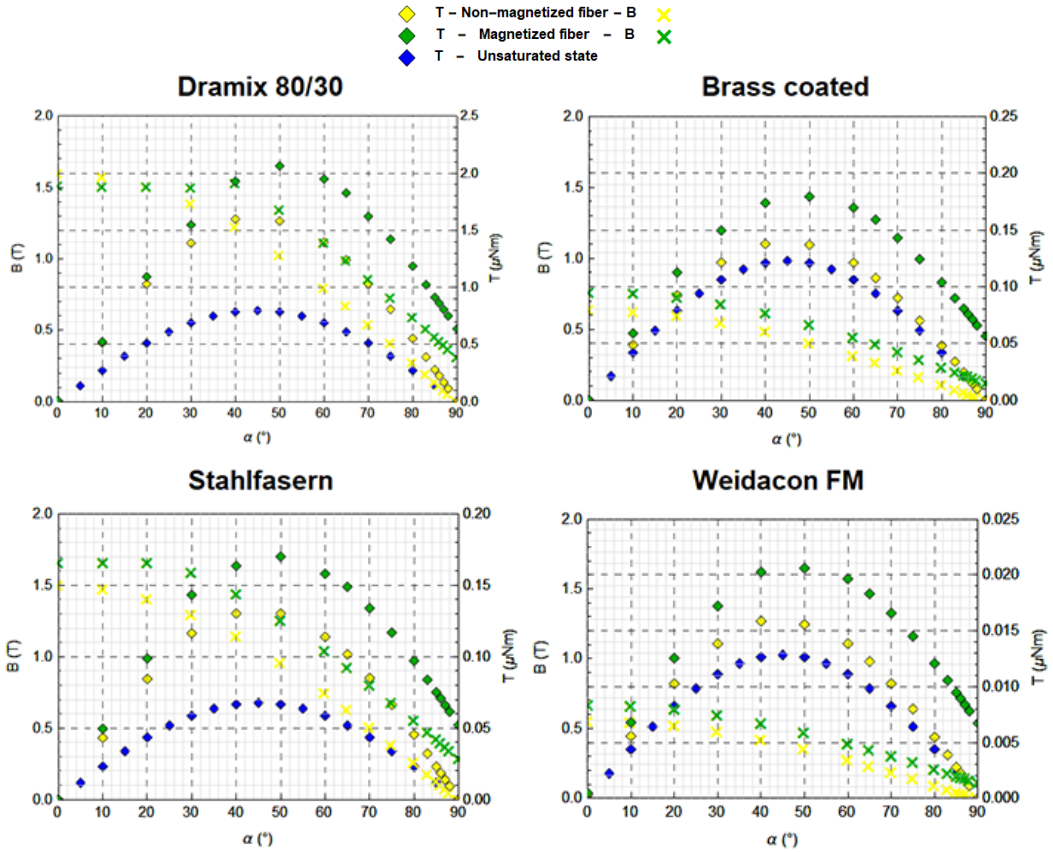

Figure 28: Torque of selected fibers - 1 mT

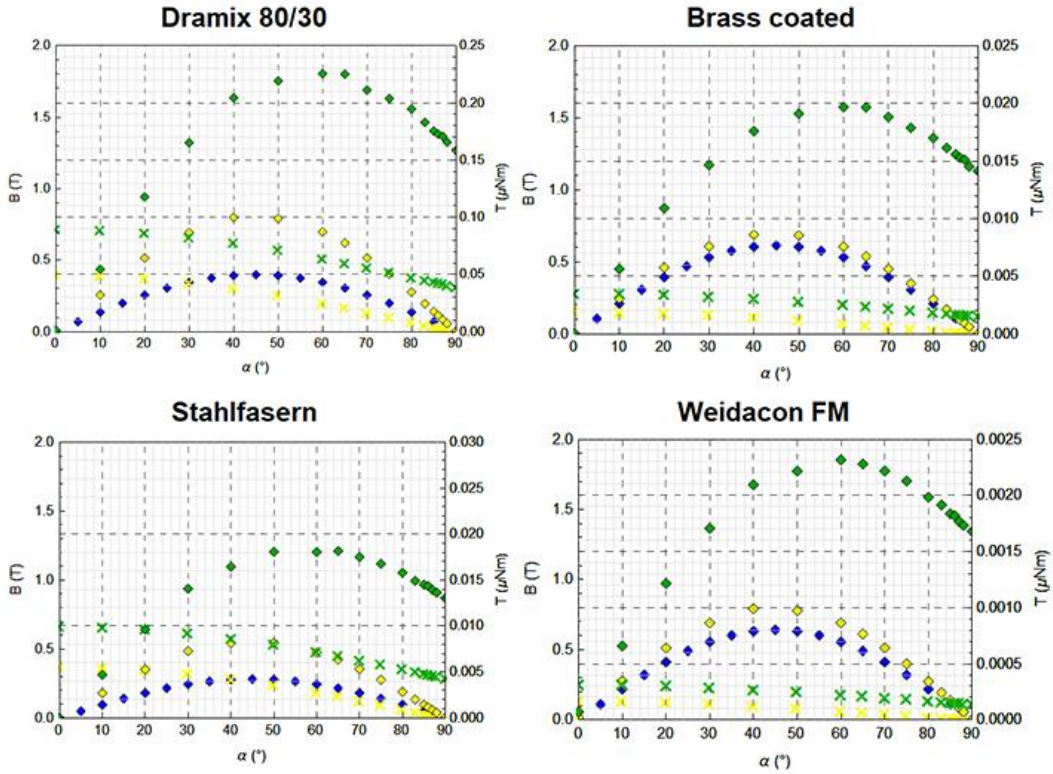

Figure 29: Torque of selected fibers - 0.25 mT

Chapter V: Conclusion

Ferromagnetic fibers used for the application of fiber-reinforced concrete allow further improvement of the mechanical properties of concrete by achieving the preferred fiber orientation using a magnetic field. Resulting composite acquires anisotropic mechanical properties in the desired direction, thus reducing the required amount of added fibers and achieving financial savings. The possibility of simulating the fiber's behavior in the magnetic field allows for a better understanding of the process of fiber's magnetic orientation.

Fibers' rotation process in the magnetic field of two coils was modeled in ANSYS (ANSYS Workbench, 2020 R1, ANSYS Inc.). A simulated dependency of fiber's torque on its position in relation to the external field is presented for a magnetized and a non-magnetized fiber's initial state, as well as for magnetic fields of various strengths. The influence of fibers' non-linear behavior in the magnetic field is shown on the measured torque characteristics.

Maximum theoretical torque for two idealized states, unsaturated and saturated, is compared to the simulated torque. This comparison shows that the maximum value of torque can be estimated for a general understanding of the torque range a fiber can produce. However, when a large amount of fibers is used in close proximity, the fibers' magnetic fields that are much stronger than the external field affect each other. During the orientation process fibers can align in chains due to attractive magnetic forces. Simulation of fibers' mutual influence can be the direction of further research.

Comparison of different commercially available fibers shows a similar behavior due to similarities in fibers' magnetization characteristics.

REFERENCES

1. Kang, S.-T.; Kim, J.-K. The relation between fiber orientation and tensile behavior in an Ultra High Performance Fiber Reinforced Cementitious Composites (UHPFRCC). Cem. Concr. Res. 2011, 41, 1001–1014. [CrossRef]
2. Ru Mu, Hui Li, Longbang Qing, Jianjun Lin, Quanming Zhao. Aligning steel fibers in cement mortar using electro-magnetic field. Construction and building materials 2016, 0950-0618. [CrossRef]
3. Lewin, W. MIT Physics II: Electricity and Magnetism. Lect 21 – Magnetic Materials, Dia- Para- & Ferromagnetism, Lect 22 – Maxwell's Equations. 2015. [CrossRef]
4. Magnetic moment. Amperian loop model. [CrossRef]
5. Domains of a ferromagnetic material. [CrossRef]
6. How the B-H Curve Affects a Magnetic Analysis. Diagram of a typical D-H curve and the corresponding differential permeability. [CrossRef]
7. Künzel, K.; Papež, V.; Carrera, K.; Konrád, P.; Mára, M.; Kheml, P.; Sovják, R. Electromagnetic Properties of Steel Fibres for Use in Cementitious Composites, Fibre Detection and Non-Destructive Testing. Materials 2021, 14, 2131. [CrossRef]
8. Dvořák, L. Magnetostatika: permanentní magnety a jejich pole. MFF UK Praha, 2020 [CrossRef]
9. MasterFieber 482 (Brass coated) fiber datasheet. [CrossRef]
10. Dramix 80/60 fiber datasheet. [CrossRef]
11. Dramix 80/30 fiber datasheet. [CrossRef]
12. Weidacon FM fiber datasheet. [CrossRef]
13. Stahlfasern fiber datasheet. [CrossRef]

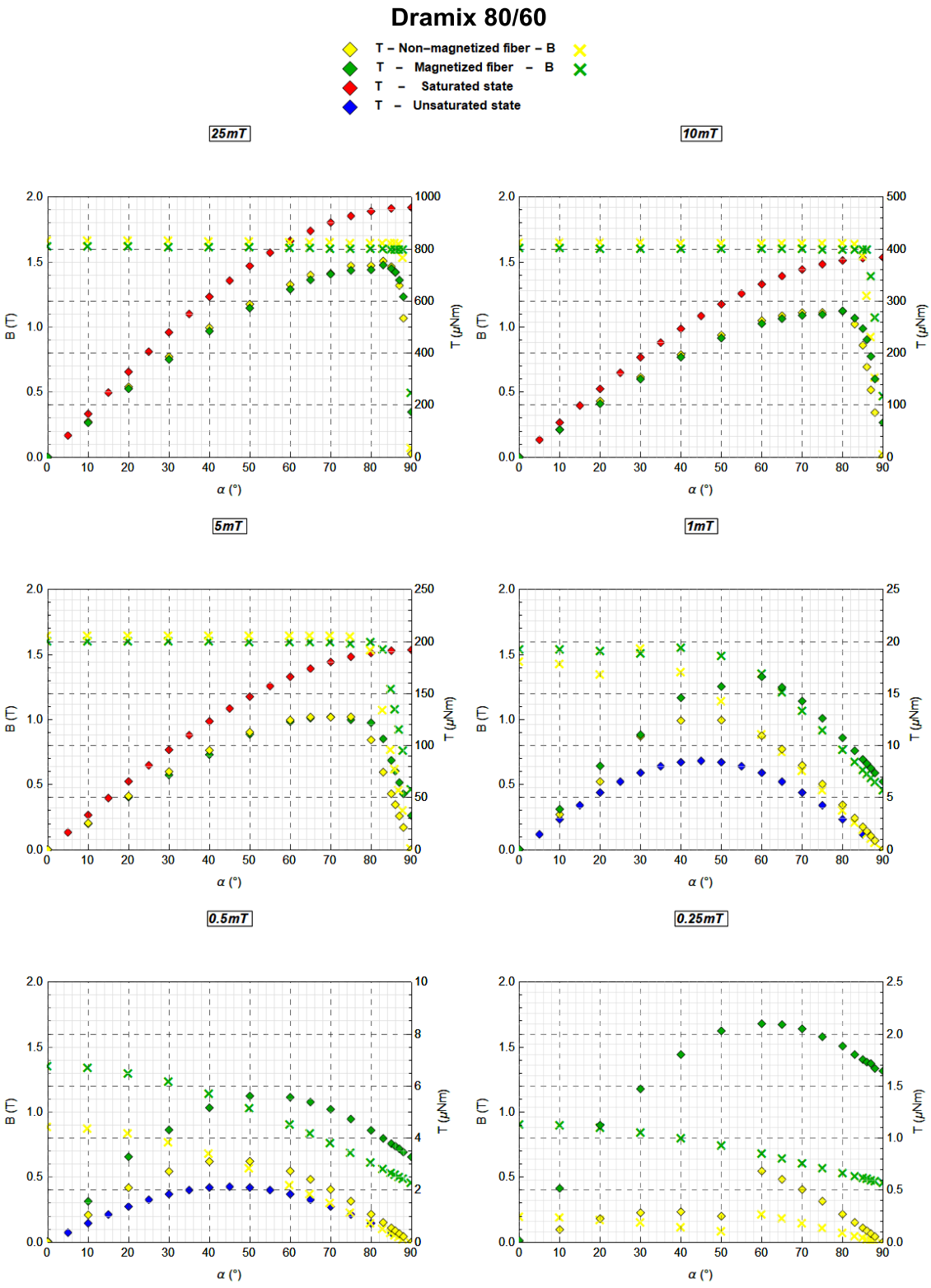
Dramix 80/60
T – Non–magnetized fiber – B
T – Magnetized fiber – B
T – Saturated state
T – Unsaturated state
25mT
10mT
5mT
1mT
0.5mT
0.25mT
B (T)
T (μNm)
α (°)

Brass coated

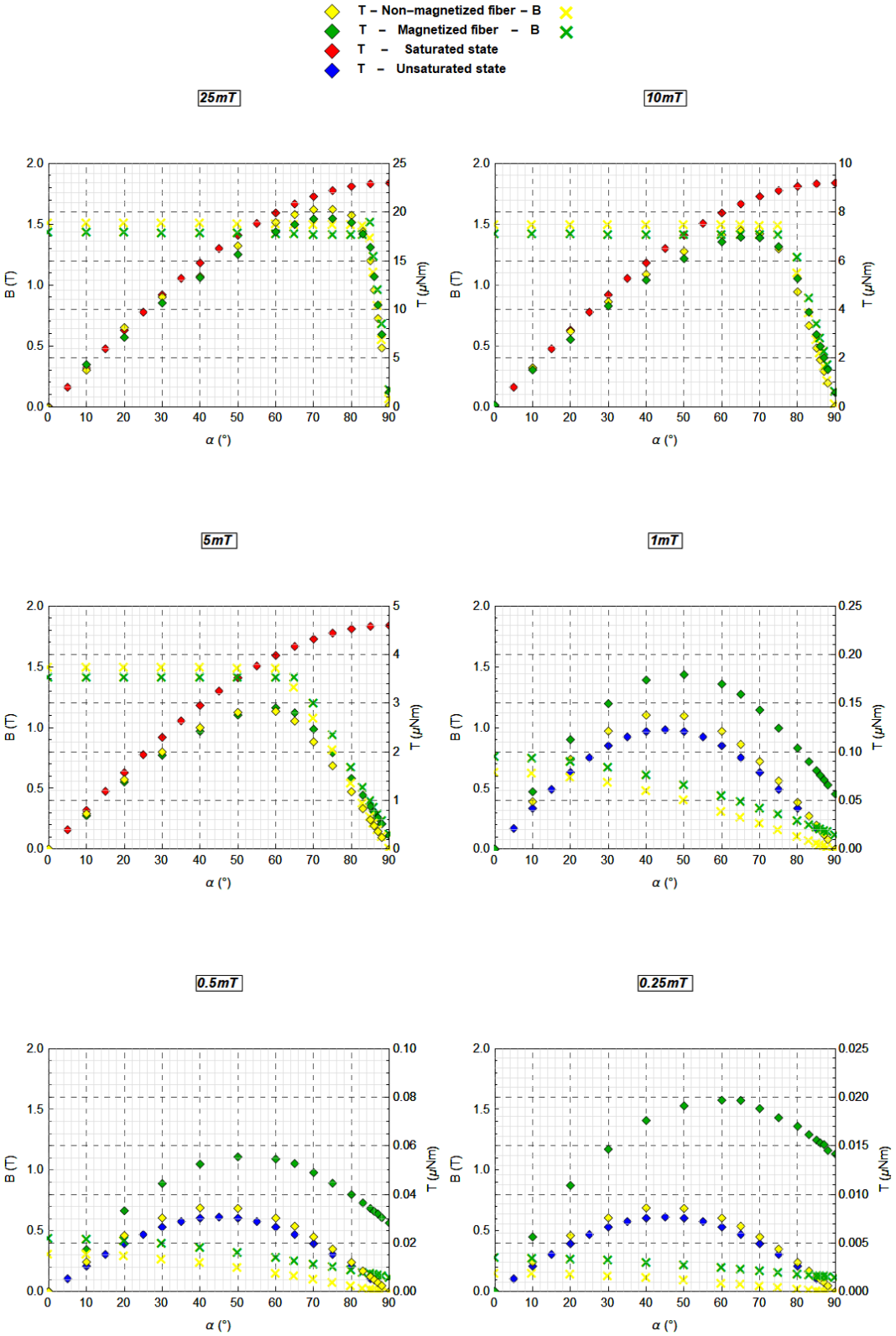

Stahlfasern

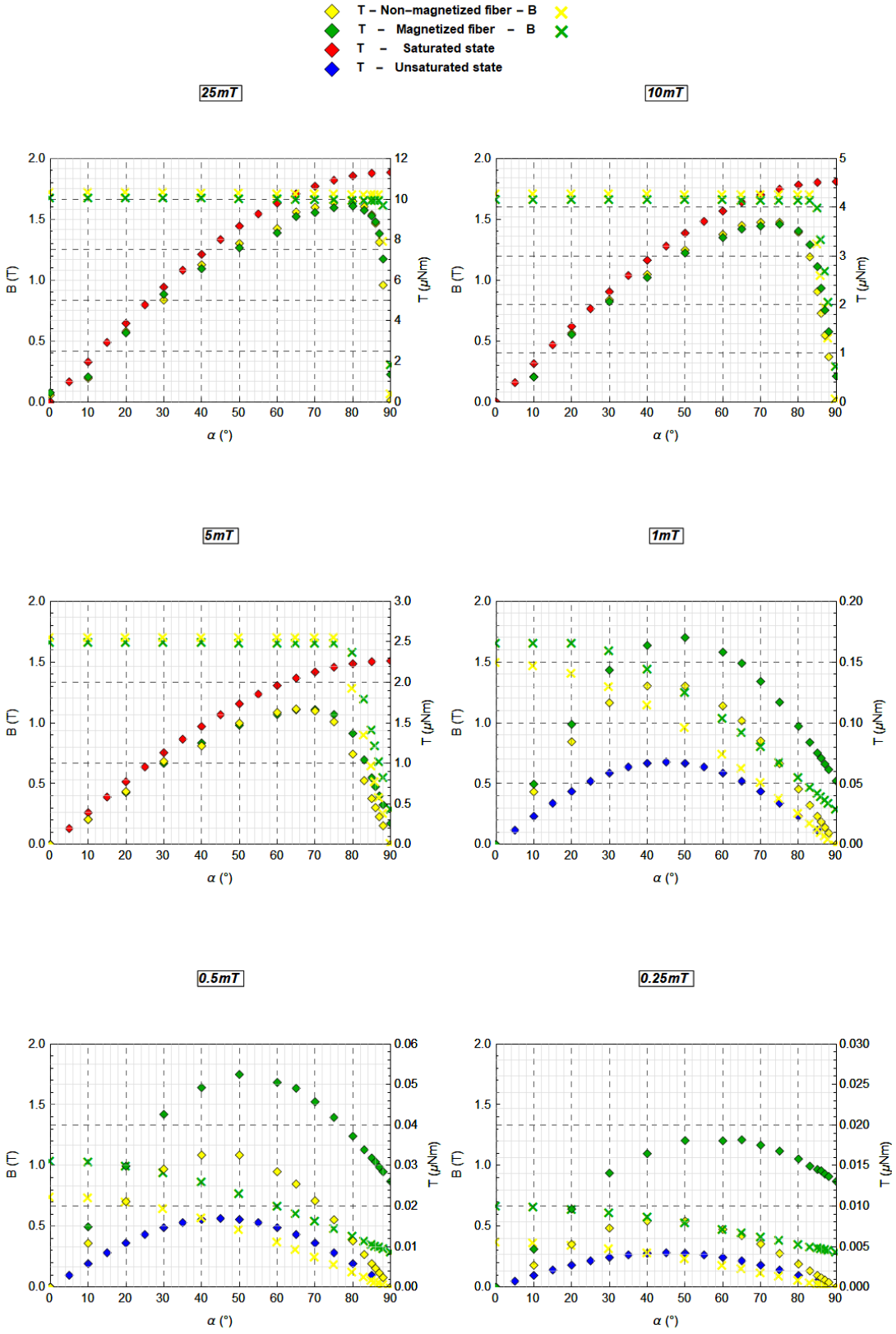

Dramix 80/30

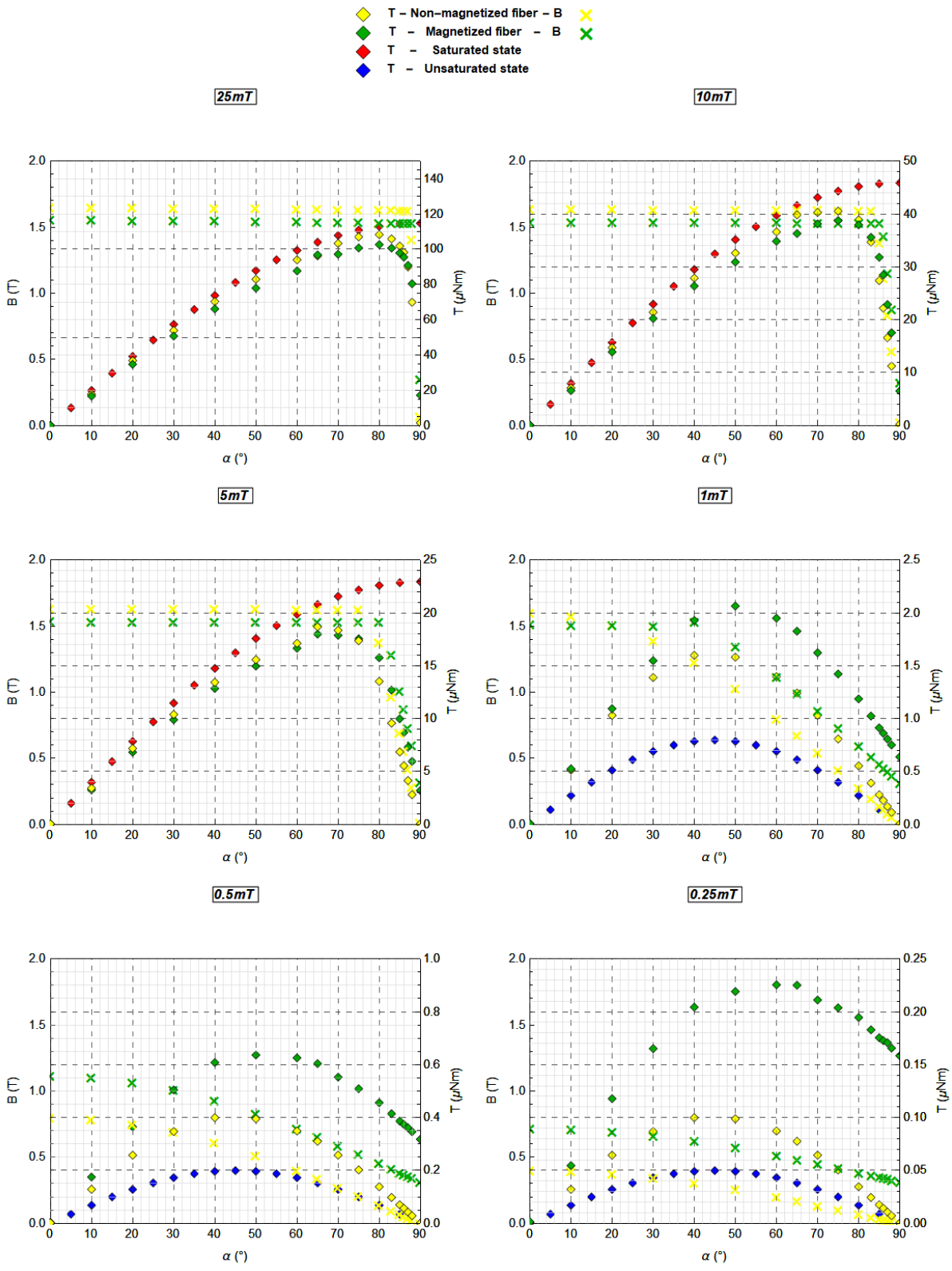
T – Non–magnetized fiber – B
T – Magnetized fiber – B
T – Saturated state
T – Unsaturated state
25mT
10mT
5mT
1mT
0.5mT
0.25mT
B (T)
T (μNm)
α (°)

Weidacon FM

T – Non–magnetized fiber – B
T – Magnetized fiber – B
T – Saturated state
T – Unsaturated state

25mT

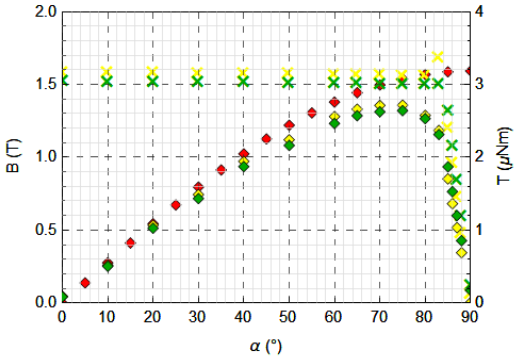

10mT

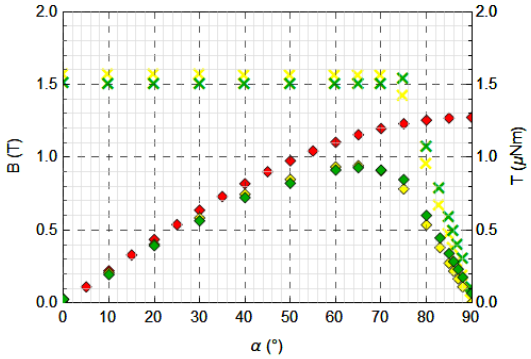

5mT

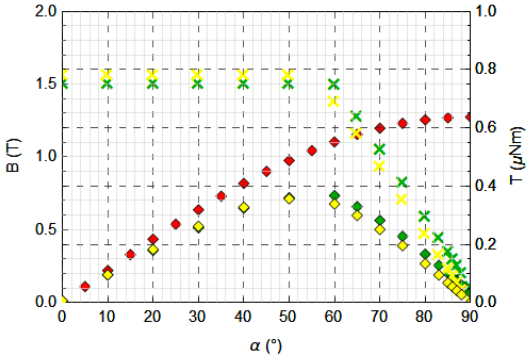

1mT

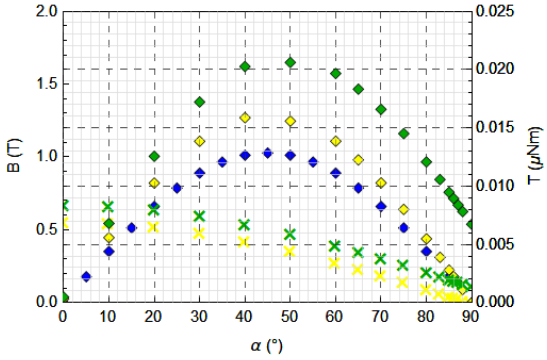

0.5mT

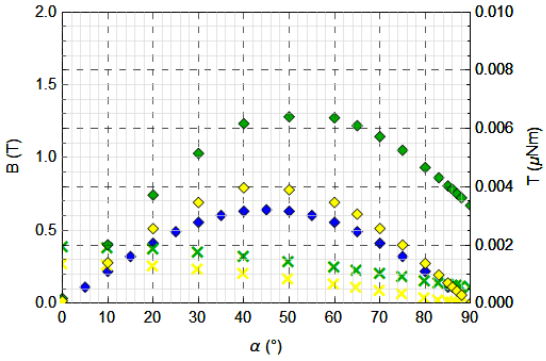

0.25mT